Response to the editor decision and the reviews, concerning the discussion paper “A multi-proxy analysis of late Quaternary Indian monsoon dynamics for the Maldives, Inner Sea”

Dorothea Bunzel et al.

Correspondence to: dorothea.bunzel@uni-hamburg.de

Dear Dr. Luc Beaufort,

with this letter we submit a revised manuscript prepared for publication in Climate of the Past. The manuscript is entitled “A multi-proxy analysis of late Quaternary Indian monsoon dynamics for the Maldives, Inner Sea” and written by D. Bunzel, G. Schmiedl, S. Lindhorst, A. Mackensen, J. Reolid, S. Romahn, and C. Betzler. The manuscript has been prepared in accordance with the instruction for authors and none of the authors have any conflicts of interest (duplicate publication, financial, etc.).

We would like to thank you for acknowledging our replies to the reviews. The two anonymous reviewers are also thanked for bringing up their suggestion and substantial comments, which helped to improve our work considerably. We have changed the text accordingly and respond to all comments raised by the reviewers on the following pages. All relevant changes made in the manuscript (addressing lines, chapters or figures) are mentioned in our responses to the corresponding reviewer comments. Additionally, we have also made some minor revisions regarding misspellings, text phrasing, formatting of the text/figures, adding more values in the result chapters etc. We also suggest to provide the data records of sediment core SO236-052-4, which we used and discussed in our manuscript, to the PANGAEA Open Access library. We mentioned it in lines 211-212 at the end of the methods.

The structure on the next pages is as follows:

- Reviewer Comments (RC)
- *Authors Responses*
- Changes in the manuscript

With kind regards (on behalf of all co-authors),
Dorothea Bunzel

Responses to Referee#1

1) **RC#1:** I don't find the title of the current manuscript really suitable. The title suggest that the Maldives record is mainly driven by "Indian monsoon dynamics" whereas the authors conclude that the record provide a close linkage between the Indian monsoon oscillation, intermediate water circulation, productivity and sea-level changes on orbital time-scale. Therefore, a title such as "A multi-proxy analysis of late Quaternary equatorial Indian ocean for the Maldives, Inner Sea" could be less confusing.

   Response: *Thank you for suggesting a more suitable title. We have adjusted the title as follows: "A multi-proxy analysis of Late Quaternary ocean and climate variability for the Maldives, Inner Sea"*

2) **RC#1:** Lines 57 to 59. There is much more references of Arabian Sea works at the orbital and suborbital time scales (Clemens et al., 1996; Altabet et al., 2002; Clemens and Prell, 2003; Pichevin et al., 2007; Boning and Bard, 2009; Ziegler et al., 2010; Caley et al., 2011; Caley et al., 2013, Deplazes et al., 2013 are some examples).

   Response: *Thank you for recommending these works; we have included the mentioned references in our revised version (now lines 47-50).*

3) **RC#1:** Lines 179-180: "Local reservoir corrections were not applied". The authors should explain why they do not applied a correction. In general a correction of 400 years is applied in the tropics.

   Response: *We did not correct our radiocarbon ages for local reservoir effects, because of the contrast between the closest available numbers of marine reservoir age corrections, which are from the Arabian Sea, Northern Indian Ocean and Bay of Bengal, and between 821 and 864 km distance from our study site. We have changed the text as follows (now lines 203-206): "Due to the contrasting available reservoir age correction values (varying between 301 to 544 years; Dutta et al., 2001; Southon et al., 2002), the AMS ^{14}C ages were corrected for the global reservoir age of 400 years in order to minimize potential errors and converted to calendar years using the radiocarbon calibration program CALIB (version 7.0.4; Stuiver and Reimer, 1993) and the calibration curve Marine13 (Reimer et al., 2013)."*

4) **RC#1:** Lines 202-209: Oxygen concentration should be shown on figure 3 and not only on Figure 8.

   Response: *We have included all full-resolution $\Delta\delta^{13}C$ data, which were used for the bottom-water oxygen reconstruction ($\Delta\delta^{13}C_{Cm-Ga}$) and water column mixing ($\Delta\delta^{13}C_{Gr-Cm}$) in Figure 3c.*

5) **RC#1:** Lines 217-221: The data of core M74/4-1143 are not shown on figure 4 making the comparison with core SO-236-052-4 impossible.

   Response: *We have included the sortable silt data of core M74/4-1143 in the Figure (Fig. 5a). Due to our additional created figures for the revised manuscript, the former Figure 4 became Figure 5 now.*

6) **RC#1:** Lines 228-233 and 258-259; Are the Fe/Ca and Si/Ca good proxies for Aeolian dust? The results could be compared to dust data from site ODP722 (Clemens et al., 1996). This is important to discuss the provenance of the dust and the interpretation of the Fe/Ca and Si/Ca that stays speculative in the discussion (lines 258-268). Also, previous study in the Arabian Sea used rather the changes in the Ti/Al ratio of the sediments as indicator for grain size and thus wind speed, since Titanium is concentrated in heavy minerals in the coarser size fraction (Reichart et al., 1997; Ziegler et al., 2010 CP).

   Response: *We consider the more commonly used proxies for terrigenous sediment delivery/aeolian dust fluxes and we have modified our manuscript as follows: We have replaced the Fe/Ca record by the Ti/Al and Fe/Al records as proxies for aeolian dust supply and enhanced aridity of the hinterland/source area (e.g. Zhang et al., 1993; Lourens et al.,* *2001; Itambi et al., 2009) in order to account for a potential influence of changes in carbonate production and preservation on the Fe/Ca ratio (Wehausen and Brumsack, 2000). We have included the Fe/Al record because the aeolian Fe flux to the ocean likely has a direct impact on the seasonal surface ocean productivity (e.g. Martin et al., 1991; Boyd et al., 2000; Gao et al., 2001; Jickells et al., 2005), which also influences the deep-sea benthic ecosystems through seasonal phytodetritus pulses. Both Ti/Al and Fe/Al records show a similar glacial-interglacial pattern with relatively higher values during cold stages corroborating the foraminiferal results of enhanced surface ocean fertilisation of the Maldives Inner Sea during glacial periods (see lines 257-260, as well as Figs. 4-5, 8). We also show and discuss the Si/Ca ratio in addition, because we argue that the increase in agglutinated benthic foraminifera is a reflection of the availability of terrestrial particles, since most of these agglutinated species preferentially use siliciclastic grains for building up their test walls (e.g., Murray, 2006).*

We have referred to the lithogenic flux record of site ODP722 (Clemens et al., 1996) since it supports our observation of generally enhanced glacial dust fluxes (for discussion see lines 298-309 and 321-323). However, we have refrained from plotting the data because of its comparatively low temporal resolution for the targeted time interval.

7) **RC#1:** Line 278: “Fe/Ca record lacks significant variability on the precession band”. Statistical analyses are necessary (spectral analyses) to confirm this point.

***Response**: For a proper statistical analysis we have now performed a Blackman-Tukey spectral analyses for the oxygen concentrations of core SO236-052 and GeoB3004, as well as for TOC, bromine, Fe/Al and Ti/Al ratios of core SO236-052 in comparison to the Δ-insolation at 30° N (for methods see chapter 2.5: Spectral analyses). Both reconstructed oxygen records reveal strong power in the precession band (23 ka period); see lines 234-235. Significant but considerably weaker variability in the precession band is also detected in the TOC, Ti/Al records and the Br XRF counts. The Fe/Al record lacks substantial precessional variability but is rather dominated by long-term glacial-interglacial changes (lines 263-265). All results of the Blackman-Tukey spectral analysis are displayed in Fig. 4.*

8) **RC#1:** Lines 336-337: “While the benthic foraminiferal fauna preliminary show changes on glacial-interglacial time scale, the TOC content and Ba/Ca ratio are characterized by additional variability in the precessional band.” Again, statistical analyses are necessary (spectral analyses) to confirm this point.

***Response**: See response to referee comment #7.*

9) **RC#1:** Lines 342-347: “Elevated TOC and Ba/Ca ratios at site SO-236-052 during phases of reduced northern hemisphere summer insolation suggest a direct influence of the Indian winter monsoon on productivity and related organic matter fluxes of the Maldives Inner Sea during the past 200 ka, which is consistent with the present-day situation (de Vos et al. 2014). The close link between the winter monsoon intensity and surface water productivity in the study area is confirmed by the difference between the δ^{13}C values of the epipelagic G. ruber (Gr) and the epibenthic C. mabahethi (Cm) (Figs. 3, 8).” Again, statistical analyses are necessary with a phase analyse. Also, what could be the role of the IEW and ENSO mentioned in the introduction part?

***Response**: With exception of the oxygen records, the TOC, Ti/Al, Fe/Al records reveal a comparatively weak coherence in the precession band (see also answer to referee comment #7). This result is likely related to the strong dominance of the 100 ka periodicity (as for example reflected in the dust supply) and superposition of shorter-wave variability. Hence, we did not include results from cross-spectral analyses.*

We have acknowledged and discussed the documented influence of IEW and ENSO variability on equatorial Indian surface ocean environments in the introduction and the discussion chapters (lines 50-60 and 478-486). On the other hand, the close relation of the present-day productivity in the Maldives Inner Sea surface waters (as reflected in seasonal satellite chlorophyll a images) to the northern hemisphere winter season clearly demonstrates a relation to the

NE monsoon of this particular area. Specifically, our proxy records suggest enhanced dust fluxes and productivity during glacial boundary conditions underlining a general affiliation of Maldives Inner Sea paleoenvironments to the NE monsoon and high-latitude climate changes (dust availability, sea-level changes). To admit, we cannot exclude a potential additional influence of changes in IEW and ENSO but a proper statistical evaluation of phase relationships in the precessional band is unfortunately inhibited by the relatively weak precessional component and coherence in our proxy records of surface water productivity (such as TOC content, Br XRF counts; see Fig. 4). But we addressed this issue in our revised manuscript in order to better acknowledge the possibility of IEW influence as observed in other studies.

10) **RC#1:** Lines 372-376: "Long-term trends of similar magnitude have been recorded from sites bathed by the Antarctic Intermediate Water mass (AAIW) in the southwestern Pacific Ocean (Pahnke and Zahn, 2005; Elmore et al., 2015; Ronge et al., 2015). The general resemblance of the various epibenthic δ^{13}C records suggests a significant role of AAIW in ventilation of bathyal environments of the Maldives Inner Sea, which is consistent with the modern oceanographic situation (You, 1998)." It would be good to add the data of the previous work mentioned on the Figure of the manuscript for a direct comparison.

   ***Response**: Thanks for raising this important point. For the revised version of our manuscript we have created an additional figure comparing our epibenthic stable carbon isotope record with the published records from the southwestern Pacific Ocean (Fig. 10): SO136/003 (Thiede et al., 1999), MD97-2120 (Pahnke and Zahn, 2005), DSDP593 (Elmore et al., 2015), MD06-2986 and MD06-2990 (Ronge et al., 2015). The general resemblance of the δ^{13}C trends from different regions confirms the super-regional AAIW influence.*

11) **RC#1:** Lines 385-386: "The reconstructed O_2 record reveals precessional changes between oxic and low oxic conditions during northern hemisphere insolation maxima and minima, respectively". Statistical analyses are necessary (spectral analyses) to confirm this point.

   ***Response**: Spectral analysis of the oxygen records reveals significant variability in the precession band (see also answer to referee comment #7 and Fig. 4a).*

12) **RC#1:** Lines 406-412: "Agulhas leakage". I do not understand this paragraph and the link with the Agulhas leakage. If the authors want to demonstrate a link between their record and the Indian monsoon they can compare directly with published monsoon records. Also, the forcing of the Agulhas leakage at terminations is driven by the subtropical front migration and is not directly link to the Indian monsoon (Peeters et al., 2004). For the IEW impact, a statistical analyze with the phase relationship (spectral analyses) will help the interpretation of the record.

   ***Response**: We admit, that the discussion related to the Agulhas leakage is not essential for the main conclusions of our paper. In order to avoid confusion, we have deleted this paragraph. For the potential IEW impact see our response to referee comment #9.*

Responses to Referee#2

1) **RC#2:** Overall, I think the analysis of the data and its presentation could be improved. Some of the statements in the discussion (e.g. correlation of certain proxies with insolation or other proxy records, glacial-interglacial cycles) is often not supported by statistics or suitable figures (see comments below).
   I am also missing clear common thread and objective. This starts already in the abstract. It's starts of with a paragraph that basically says : "We measured a lot of stuff on a sediment core in the Maldives region. . .and then we interpreted the data..". I think it would be much more appealing if the manuscript would start with the context of the study, the main research question or problem or a hypothesis. Then they should list their approach (multi-proxy approach)
   ***Response**: Thank you for your suggestions. In the revised version we have included results from Blackman-Tukey spectral analysis in order to evaluate the variability in the precession band (see chapter 2.5: Spectral analyses). For a proper statistical evaluation of long-term variations (i.e., in the eccentricity band) our time series is too short. Our conclusions on the general glacial-interglacial variability are therefore still based on the graphical correlation among proxy records.*
   We rewrote the first part of the abstract addressing the relevance and principal objectives of our study, and explaining why we selected the particular study area (see lines 9-15).

2) **RC#2:** I think the paragraph from line 57 to line 66 could be improved. This paragraph contains a controversy in the interpretation of past OMZ variability in the Arabian Sea and its relation with summer monsoon variability. Is a strong OMZ linked to increased productivity (monsoon driven upwelling) or reduced ventilation (lower oxygen conc in southern sourced intermediate waters). The study by Bundel et al could inform this debate by providing a record of oxygen concentration from further South. There are some records (e.g. Ziegler et al., 2010, Climate of the Past) that show that a deep (most extended) OMZ occurs during glacial periods. While productivity maxima in the Arabian Sea, occur during interglacials. The new data by Bundel et al., could help to explain this observation by proving constraints of the Arabian Sea intermediate water ventilation from the South.
   ***Response**: According to the existing data and also supported by our new record, the OMZ in the northern Indian Ocean is controlled by both changes in ventilation of intermediate (central OMZ; Das et al., in press 2017) and deep-water masses (deep OMZ; see Schmiedl and Leuschner, 2005; Ziegler et al., 2010), and by regional oxygen consumption responding to upwelling-driven high surface productivity (e.g., Reichart et al., 1998; Das et al., in press 2017). Our reconstruction corroborates this conclusion as it shows the general presence of an OMZ, which is also preconditioned by the biogeochemical processes in the Arabian Sea. The observation of generally reduced oxygen concentrations during glacial boundary conditions (particularly during MIS 4-2) reflects the ventilation signal of southern-derived intermediate water although with a probable regional signal of winter-monsoon-induced enhanced organic matter fluxes and oxygen consumption. The combination of the different factors (intermediate water circulation, summer and winter monsoon influence in different regions) have been emphasized and the discussion clarified in the revised manuscript; see e.g. lines 88-93 and 449-459.*

3) **RC#2:** Line 64: studies in stead of studied?
   ***Response**: All identified misspellings have been corrected in the revised manuscript. The former sentences (lines 61-66, respectively) have been summarized (now lines 88-91).*

4) **RC#2:** line 77 -82: This section lists the main objectives of the study. Its strange that the objectives 1 and 2 mention suddenly, dust flux and sea-level, while the entire introduction does not mention either of the two. I would focus on objective 3 and mention the subjects that deal with 1 and 2 in the discussion without putting to much emphasis on it.

***Response**: We agree that the role of sea-level and dust fluxes is underrepresented in the introduction. Our proxy records highlight both changes in sea-level and dust fluxes as relevant factors for sedimentation and marine ecosystem dynamics in the Maldives, Inner Sea. Therefore, we have enhanced the introduction chapter including a new paragraph providing background information on the influence of these parameters in the wider study area (lines 61-77).*

5) **RC#2:** line170: "... .are based on. . ."

   ***Response**: It has been corrected (line 190).*

6) **RC#2:** line 173: 'was estimated to assess.."

   ***Response**: It has been corrected (line 192).*

7) **RC#2:** line 179-180: Why was a local reservoir age not applied?

   ***Response**: See response to referee#1, comment #3, and the supplement we have made in the revised manuscript: lines 203-206.*

8) **RC#2:** line 224: Given that the authors did XRF scanning, they should also have Bromine data. Bromine has been used successfully in several studies in the Indian Ocean as organic matter indicator (Caley et al., 2013, QSR, Ziegler et al, 2008, G3). The authors could do the same to get a high-resolution organic matter record and get a better idea of short term variability in TOC.

   ***Response**: Thank you for this suggestion. We have checked the bromine XRF counts in relation to the measured TOC values. Both data records reflect the same pronounced glacial-interglacial pattern with high values during glacial periods, but also reveal additional variability in the precession band over the studied time period (Figs. 4c-d, 8b-c). In the revised manuscript we have replaced the Ba/Ca record by the Br XRF counts and evaluated the latter statistically (Blackman-Tukey spectral analysis, chapter 2.5).*

9) **RC#2:** line 258-260: What about the possibility that Fe/Ca and Si/Ca reflect changes in carbonate production / preservation? Maybe the dust input has been constant through time? See also related comments by the other reviewer. I fully agree with him.

   ***Response**: We agree since we cannot exclude potential changes in carbonate production. Therefore, we have included Ti/Al and Fe/Al instead of Fe/Ca as aeolian dust proxies (see also answer to referee#1, comment #6). However, we still display and discuss the Si/Ca record since it reflects the availability of siliciclastic grains in the sediment for test construction of agglutinating foraminiferal species (see lines 125-129 for all XRF proxy records used in the revised manuscript).*

10) **RC#2:** line 278: at the precessional band

    ***Response**: It has been corrected (line 312).*

11) **RC#2:** line 282: There are several studies that suggest that late Pleistocene quasi-100 kyr cycles are not driven by eccentricity, but instead are a response to skipped precession and/or obliquity cycles

    ***Response**: For a statistically more robust evaluation of the full orbital variability (including the long-wave components) in our data series we would need a time series, which is considerably longer than 200 ka. Nevertheless, graphical comparison of our data series reveals pronounced glacial-to-interglacial changes suggesting a link to eccentricity-driven environmental changes (e.g. Fig. 8). Our conclusions are also in line with dust flux reconstructions from the Arabian Sea (e.g., Clemens et al., 1996) which show striking changes on the glacial-to-interglacial timescale (in the* *eccentricity band) suggesting a close link to environmental changes and associated dust availability on the northern borderlands. While the eccentricity component appears dominant in the dust proxies, variability in the precession band seems to be considerably lower (as indicated by spectral analyses; see Fig. 4). We considered and discussed these results in the revised version (e.g. lines 313-317 and 321-323).*

12) **RC#2:** line 342-345: I don't see a correlation of TOC or Ba with summer insolation. This should be demonstrated in a figure.
Response*: In the revised version of figure 8 (former Fig. 7) we have displayed the Br XRF counts (see comment above) and TOC as indicators for productivity together with the difference of the summer and winter insolation at 30° N, which enables a graphical correlation of the mentioned proxy records and northern hemisphere insolation. This comparison reveals coherent glacial-to-interglacial changes in the TOC and Br record (also in the Ba/Ca record) with elevated values during glacial stages MIS 6 and MIS 4-2. For a statistical evaluation of the relation between insolation and the TOC and Br records we have performed a Blackman-Tukey spectral analyses and have presented the power spectra in a new figure (Fig. 4).*

13) **RC#2:** section 4.2: This section seems not to be very important in the context of the whole manuscript. I would therefore again suggest to omit the sea-level topic from the list of main objectives.
Response*: We are convinced that sea-level changes exert a strong impact on sedimentation processes and paleoenvironmental conditions of the Maldives Inner Sea. This is clearly reflected by the composition of the benthic foraminiferal fauna (e.g. assemblage 1, meroplanktonic taxa) and other parameters, such as the Sr/Ca ratio and grain size etc. We therefore did not omit this process from the main objectives. Instead, we provide a bit more background on the relation between sea-level and the sedimentary system/paleoenvironment of the Maldives in the introduction chapter (see also comment above, and lines 73-79).*

14) **RC#2:** line 370-376: show the comparison with other datasets also in the figures otherwise the reader cannot judge your arguments
Response*: We agree with this suggestion. We have created an additional figure for the epibenthic stable carbon isotope records (Fig. 10), which enables the comparison of our data with published data (Thiede et al., 1999; Pahnke and Zahn, 2005; Elmore et al., 2015; Ronge et al., 2015). See also our answer to referee#1, comment #10).*

15) **RC#2:** line 388-390: This sentence seems to contain a contradiction. Is the Maldives OMZ controlled by expansion of the Arabian Sea OMZ are controlled by the ventilation of southern sourced waters. (I would think it is the latter)
Response*: The present OMZ of the northwestern Indian Ocean extends from the northern Arabian Sea into the tropical Indian Ocean (Reid, 2003) reflecting the reduced ventilation of intermediate water masses (due to its remote position) and the biogeochemical processes related to monsoon-induced organic matter fluxes and decomposition. We therefore assume that the OMZ variability in the Maldives Inner Sea is influenced by the overall strength and lateral expansion of the Arabian Sea OMZ, but it is additionally controlled by the ventilation of southern-derived oxygen-rich intermediate waters (AAIW) and by local monsoon-related organic matter fluxes and oxygen consumption. The general resemblance of our epibenthic stable carbon isotope record with comparable records from other areas indicates an ocean-wide link of intermediate water ventilation. On the other hand, the significant variability of our new oxygen reconstruction from the Maldives Inner Sea in the precession band and its resemblance with the reconstruction from the Arabian Sea suggests an additional influence of monsoon-driven biogeochemical processes. We have clarified the text accordingly (e.g. lines 444-459).*

16) **RC#2:** line 396-401: I would argue the other way around. Low oxygen conc in intermediate waters in the Maldives area preconditioned the waters that ventilate the Arabian Sea. So a deep Arabian Sea OMZ has its root in the central Indian Ocean (and is thus not exclusively controlled by monsoon variability).

    Response*: see also comment above. The oxygen concentrations in the northwestern Indian Ocean display a gradient with very low values in the northern Arabian Sea and increasing values to the South. This gradient illustrates a clear relation to the monsoon-related biogeochemical processes in the Arabian Sea, but is also a reflection of the remote position of the Arabian Sea in terms of intermediate water ventilation. Nevertheless, a monsoon-induced strengthening of the OMZ in the Arabian Sea (as during MIS 3) will results in an increase of the north-south oxygen gradient in the entire northwestern Indian Ocean, which should then also be detected in the Maldives Inner Sea (although at a lower amplitude). See lines 471-477.*

17) **RC#2:** line 428: demonstrate cyclicality through spectral analysis (see also comment by other reviewer, fully agree)

    Response*: We have performed Blackman-Tukey spectral analyses and have included the results in the revised manuscript. See also answer to referee#1, comment #7, and chapter 2.5.*

18) **RC#2:** Figure 6: Why is assemblage 2 abundant in the glacial MIS 6 and the Holocene? (Why is assemblage 1 abundant in 5, but absent in the Holocene)?

    Response*: This is a good question, but we do not yet have a simple explanation for it. Obviously, glacial conditions during MIS 6 were different from MIS 4-2 (Dansgaard et al., 1993); the latter was characterized by relatively lower sea-level and more intense glacial boundary conditions.*

    Previous studies showed similar patterns, with certain benthic foraminiferal assemblages occurring both during glacial and interglacial periods, e.g. in the Red Sea (Badawi et al., 2005). At the Maldives Inner Sea, glacial-to-interglacial changes in food fluxes were likely not extreme and therefore ecological thresholds for certain species and faunas may not have always been passed during glacial-interglacial transitions. A detailed inspection of assemblage 2 (C. mabahethi-fauna) actually displays faunal differences between their occurrences in MIS 1 and MIS 6 although C. mabahethi is the dominant taxon in both intervals. For discussion of the inconsistent association of certain assemblages see also lines 379-387.

References mentioned above

Altabet, M. A., Higginson, M. J., and Murray, D. W.: The effect of millennial-scale changes in Arabian Sea denitrification on atmospheric CO_2*, Nature, 415, 159–162, doi:10.1038/415159a, 2002.*

Badawi, A., Schmiedl, G., and Hemleben, C.: Impact of late Quaternary environmental changes on deep-sea benthic foraminiferal faunas of the Red Sea, Marine Micropaleontology, 58, 13–30, doi:10.1016/j.marmicro.2005.08.002, 2005.

Böning, P. and Bard, E.: Millennial/centennial-scale thermocline ventilation changes in the Indian Ocean as reflected by aragonite preservation and geochemical variations in Arabian Sea sediments, Geochimica et Cosmochimica Acta, 73, 6771–6788, doi:10.1016/j.gca.2009.08.028, 2009.

Boyd, P. W., Watson, A. J., Law, C. S., Abraham, E. R., Trull, T., Murdoch, R., Bakker, D. C. E., Bowie, A. R., Buesseler, K. O., Chang, H., Charette, M., Croot, P., Downing, K., Frew, R., Gall, M., Hadfield, M., Hall., J., Harvey, M., Jameson, G., LaRoche, J., Liddicoat, M., Ling, R., Maldonado, M. T., McKay, R. M., Nodder, S., Pickmere, S., Pridmore, R., Rintoul, S., Safi, K., Sutton, P., Strzepek, R., Tanneberger, K., Turner, S., Waite, A., and Zeldis, J.: A mesoscale phytoplankton bloom in the polar Southern Ocean simulated by iron fertilization, Nature, 407, 695–702, doi:10.1038/35037500, 2000.

Caley, T., Zaragosi, S., Bourget, J., Martinez, P., Malaizé, B., Eynaud, F., Rossignol, L., Garlan, T., and Ellouz-Zimmermann, N.: Southern Hemisphere imprint for Indo-Asian summer monsoons during the last glacial period as revealed by Arabian Sea productivity records, Biogeosciences, 10, 7347–7359, doi:10.5194/bg-10-7347-2013, 2013.

Clemens, S. C., Murray, D. W., and Prell, W. L.: Nonstationary Phase of the Plio-Pleistocene Asian monsoon, Science, 274, 943–948, 1996.

Dansgaard, W., Johnsen, S. J., Clausen, H. B., Dahl-Jensen, D., Gundestrup, N. S., Hammer, C. U., Hvidberg, C. S., Steffensen, J. P., Sveinbjörnsdottir, A. E., Jouzel, J., and Bond, G.: Evidence for general instability of past climate from a 250-kyr ice-core record, Nature, 364, 218–220, 1993.

Das, M., Singh, R. K., Gupta, A. K., and Bhaumik, A. K.: Holocene strengthening of the oxygen minimum zone in the northwestern Arabian Sea linked to changes in intermediate water circulation or Indian monsoon intensity? Palaeogeography, Palaeoclimatology, Palaeoecology, doi:10.1016/j.palaeo.2016.10.035, in press 2017.

Deplazes, G., Lückge, A., Peterson, L. C., Timmermann, A., Hamann, Y., Hughen, K. A., Röhl, U., Laj, C., Cane, M. A., Sigman, D. M., and Haug, G. H.: Links between tropical rainfall, and North Atlantic climate during the last glacial period, Nature Geoscience, 6, 213–217, doi:10.1038/NGEO1712, 2013.

Dutta, K., Bhushan, R., and Somayajulu, B. L. K.: ΔR Correction Values for the Northern Indian Ocean, Radiocarbon, 43, 483–488, doi:10.1017/S0033822200038376, 2001.

Elmore, A. C., McClymont, E. L., Elderfield, H., Kender, S., Cook, M. R., Leng, M. J., Greaves, M., and Misra, S.: Antarctic Intermediate Water properties since 400 ka recorded in infaunal (Uvigerina peregrina) and epifaunal (Planulina wuellerstorfi) benthic foraminifera, Earth and Planetary Science Letters, 428, 193–203, doi:10.1016/j.epsl.2015.07.013, 2015.

Gao, Y., Kaufman, Y. J., Tanré, D., Kolber, D., and Falkowski, P. G.: Seasonal Distribution of Aeolian Iron Fluxes to the Global Ocean, Geophysical Research Letters, 28, 29–32, 2001.

Itambi, A. C., von Dobeneck, T., Mulitza, S., Bickert, T., and Heslop, D.: Millennial-scale northwest African droughts related to Heinrich events and Dansgaard-Oeschger cycles: Evidence in marine sediments from offshore Senegal, Paleoceanography, 24, PA1205, 1–16, doi:10.1029/2007PA001570, 2009.

Jickells, T. D., An, Z. S., Andersen, K. K., Baker, A. R., Bergametti, G., Brooks, N., Cao, J. J., Boyd, P. W., Duce, R. A., Hunter, K. A., Kawahata, H., Kubilay, N., LaRoche, J., Liss, P. S., Mahowald, N., Prospero, J. M., Ridgwell, A. J., Tegen, I., and Torres, R.: Global Iron Connections Between Desert Dust, Ocean Biogeochemistry, and Climate, Science, 308, 67–71, doi:10.1126/science.1105959, 2005.

Lourens, L. J., Wehausen, R., and Brumsack, H.-J.: Geological constraints on tidal dissipation and dynamical ellipticity of the Earth over the past three million years, Nature, 409, 1029–1033, doi:10.1038/35059062, 2001.

Martin, J. H., Gordon, R. M., and Fitzwater, S. E.: The case for iron, Limnology and Oceanography, 36, 1793–1802, 1991.

Murray, J. W.: Ecology and Applications of Benthic Foraminifera, Cambridge University Press, 1–426, 2006.

Pahnke, K. and Zahn, R.: Southern hemisphere water mass conversion with North Atlantic climate variability, Science, 307, 1741–1746, doi:10.1126/science.1102163, 2005.

Reichart, G. J., Lourens, L. J., and Zachariasse, W. J.: Temporal variability in the northern Arabian Sea Oxygen Minimum Zone (OMZ) during the last 225,000 years, Paleoceanography, 13, 607–621, doi:10.1029/98PA02203, 1998.

Reid, J. L.: On the total geostrophic circulation of the Indian Ocean: flow patterns, tracers, and transports, Progress in Oceanography, 56, 137–186, doi:10.1016/S0079-6611(02)00141-6, 2003.

Pichevin, L., Bard, E., Martinez, P., and Billy, I.: Evidence of ventilation changes in the Arabian Sea during the late Quaternary: Implication for denitrification and nitrous oxide emission, Global Biogeochemical Cycles, 21, GB4008, 1–12, doi:10.1029/2006GB002852, 2007.

Ronge, T. A., Steph, S., Tiedemann, R., Prange, M., Merkel, U., Nürnberg, D., and Kuhn, G.: Pushing the boundaries: Glacial/interglacial variability of intermediate and deep waters in the southwest Pacific over the last 350,000 years, Paleoceanography, 30, 23–38, doi:10.1002/2014PA002727, 2015.

Schmiedl, G. and Leuschner, D. C.: Oxygenation changes in the deep western Arabian Sea during the last 190,000 years: Productivity versus deepwater circulation, Paleoceanography, 20, PA2008, 1–14, doi:10.1029/2004PA001044, 2005.

Southon, J., Kashgarian, M., Fontugne, M., Metivier, B., and Yim, W. W.-S.: Marine Reservoir Corrections for the Indian Ocean and Southeast Asia, Radiocarbon, 44, 167–180, doi:10.1017/S0033822200064778, 2002.

Stuiver, M. and Reimer, P. J.: Extended ^{14}C data base and revised CALIB 3.0 ^{14}C age calibration program, Radiocarbon, 35, 215–230, 1993.

Wehausen, R. and Brumsack, H.-J.: Chemical cycles in Pliocene sapropel-bearing and sapropel-barren eastern Mediterranean sediments, Palaeogeography, Palaeoclimatology, Palaeoecology, 158, 325–352, doi:10.1016/S0031-0182(00)00057-2, 2000.

Ziegler, M., Jilbert, T., de Lange, G., Lourens, L. J., and Reichart, G.-J.: Bromine counts from XRF scanning as an estimate of the marine organic carbon content of sediment cores, Geochemistry, Geophysics, Geosystems, 9, 1–6, doi:10.1029/2007GC001932, 2008.

Ziegler, M., Lourens, L. J., Tuenter, E., and Reichart, G.-J.: High Arabian Sea productivity conditions during MIS 13 – odd monsoon event or intensified overturning circulation at the end of the Mid-Pleistocene transition?, Climate of the past, 6, 63–76, 2010.

Zhang, X., Arimoto, R., An, Z., Chen, T., Zhang, G., Zhu, G., and Wang, X.: Atmospheric trace elements over source regions for Chinese dust: concentrations, sources and atmospheric depositions on the Loess Plateau, Atmospheric Environment, 27A, 2051–2067, doi:10.1016/0960-1686(93)90277-6, 1993.

A multi-proxy analysis of Late Quaternary ocean and climate variability for the Maldives, Inner Sea

Dorothea Bunzel[1], Gerhard Schmiedl[1], Sebastian Lindhorst[1], Andreas Mackensen[2], Jesús Reolid[1], Sarah Romahn[1], Christian Betzler[1]

[1]Center for Earth System Research and Sustainability (CEN), Institute for Geology, University of Hamburg, Hamburg, D-20146, Germany
[2]Alfred Wegener Institute (AWI), Helmholtz Centre for Polar and Marine Research, Bremerhaven, D-27568, Germany

Correspondence to: Dorothea Bunzel (dorothea.bunzel@uni-hamburg.de)

Abstract. As a natural sediment trap, marine sediments of the sheltered central part of the Maldives Inner Sea represent an exceptional archive for paleoenvironmental and climate changes of the equatorial Indian Ocean. To evaluate the complex interplay between high-latitude and monsoonal climate variability, related dust fluxes, and regional oceanographic responses, we focused on Fe/Al, Ti/Al and Si/Ca ratios as proxies for terrigenous sediment delivery, and total organic carbon (TOC) and Br XRF counts as proxies for marine productivity. Benthic foraminiferal fauna distributions, grain size, and stable δ^{18}O and δ^{13}C data were used for evaluating changes in the benthic ecosystem, as well as changes in the intermediate water circulation, bottom water current velocity and oxygenation.

Our multi-proxy data record reveals an enhanced dust supply during the glacial intervals, causing elevated Fe/Al and Si/Ca ratios, an overall coarsening of the sediment and an increasing amount of agglutinated benthic foraminifera. The enhanced dust fluxes can be attributed to higher dust availability in the Asian desert and loess areas and its transport by intensified winter monsoon winds during glacial conditions. These combined effects of wind-induced mixing of surface waters and dust fertilisation during the cold phases resulted in an increased surface-water productivity and related organic carbon fluxes. Thus, the development of highly diverse benthic foraminiferal faunas with certain detritus and suspension feeders were fostered. The difference in the δ^{13}C signal between epifaunal and deep infaunal benthic foraminifera reveals intermediate water oxygen concentrations between approximately 40 and 100 µmol kg^{-1} during this time. The precessional fluctuation pattern of oxygen changes resembles that from the deep Arabian Sea, suggesting an expansion of the Oxygen Minimum Zone (OMZ) from the Arabian Sea into the tropical Indian Ocean with a probable regional signal of strengthened winter-monsoon-induced organic matter fluxes and oxygen consumption, and further controlled by the varying inflow intensity of the Antarctic Intermediate Water (AAIW). In addition, the bottom water oxygenation pattern of the Maldives Inner Sea reveals a long phase of reduced ventilation during the last glacial period. This process is likely linked to the combined effects of generally enhanced oxygen consumption rates during high-productivity phases, reduced AAIW production, and the restriction of upper bathyal environments of the Inner Sea during sea-level lowstands. Thus, our multi-proxy record reflects a close linkage between the Indian monsoon oscillation, intermediate water circulation, productivity and sea-level changes on orbital time-scale.

1 Introduction

Sedimentation and biogeochemical processes of the tropical and subtropical northern Indian Ocean are closely linked to the intensity and seasonal changes of the Indian monsoon system. From June to October, the region is dominated by the southwestern (SW) monsoon, while the northwestern (NE) monsoon operates from December to April (Wyrtki, 1973; Schott and McCreary, 2001). During the SW monsoon, coastal and open-ocean upwelling results in maximum surface water productivity and related organic matter fluxes in the Arabian Sea (Nair et al., 1989, Rixen et al., 1996). At the same time, the Southwest Monsoon Current (SMC) transports high-saline surface waters from the Arabian Sea into the equatorial region (Schott and McCreary, 2001). The SW summer monsoon variability is strongly coherent over the precessional band and reveals a close but lagged response to northern hemisphere summer insolation maxima (Clemens and Prell, 2003). In comparison, during the NE winter monsoon the ocean current system reverses and the Northeast Monsoon Current (NMC) transports lower-saline surface waters from the Bay of Bengal into the western Indian Ocean. Thus, during the NE monsoon, elevated chlorophyll *a* concentrations are mainly restricted to the Indian west coast and the Maldives area, while chlorophyll *a* strongly decrease in the Arabian Sea at the same time (Sasamal, 2007; de Vos et al., 2014; NASA MODIS-Aqua, 2014).

Evaluations of deep-sea sediment archives from the Arabian Sea delivered not only comprehensive information on the pacing and intensity of the Indian summer monsoon on orbital time scales (Clemens and Prell, 1990; Clemens et al., 1991; Clemens et al., 1996; Clemens and Prell, 2003; Ziegler et al., 2010; Caley et al., 2011a), but also show variance within orbital bands to more rapid climate shifts on suborbital time scale (Schulz et al., 1998; Altabet et al., 2002; Gupta et al., 2003; Pichevin et al., 2007; Böning and Bard, 2009; Caley et al., 2013; Deplazes et al., 2013). Records from the equatorial Indian Ocean provide a more diverse and partly contradictory picture since this region is not only influenced by the summer and winter monsoons but also by the strength of Indian Ocean Equatorial Westerlies (IEW), which are stronger during the intermonsoon seasons in spring and fall and are inversely related to the Indian Ocean Dipole (Hastenrath et al., 1993; Beaufort et al., 2001). Variations in surface water properties at a site close to the Maldives platform revealed maximum productivity at times of enhanced winter monsoon winds associated with precessional maxima in ice volume (Rostek et al., 1997). By contrast, an upper-bathyal benthic foraminiferal record from the Maldives Ridge suggests that Late Quaternary changes in organic matter fluxes are either driven by summer monsoon winds (Sarkar and Gupta, 2009) or linked to changes in the IEW strength (Sarkar and Gupta, 2014). The precessional variability in productivity records from the equatorial Indo-Pacific Ocean has been attributed to the influence of low-latitude insolation on the IEW strength and on long-term dynamics of the El Niño-Southern Oscillation (ENSO) (Beaufort et al., 1997, 2001).

The seasonal reversing circulation pattern of the modern monsoon system established ~12.9 Ma ago, as indicated by the onset of drift deposition in the Maldives Inner Sea (Betzler et al., 2016). Whereas, early aeolian dust deposits at the Maldives between ~20-12.9 Ma can be attributed to a weak proto-monsoon, when prevailing wind systems were strong enough to transport dust material into the northern Indian Ocean, but not sufficient strong to promote the water currents that generate drift deposits (Aston et al., 1973; Guo et al., 2002; Grand et al., 2015; Betzler et al., 2016). Since the early Miocene, the deposition of aeolian particles to the Maldives increased stepwise, coinciding with the onset of Asian desertification derived from loess deposits in northern China (Guo et al., 2002; Betzler et al., 2016). On a regional scale, these changes in aridity were caused by various factors, comprising the Tibetan-Himalayan plateau uplift, which intensified 25-20 Ma ago, and changed wind circulation patterns due to the uplifted topography (Ruddiman and Kutzbach, 1989; Manabe and Broccoli, 1990; Harrison et al., 1992; Guo et al., 2002). However, little detailed information is available about the variability of aeolian dust delivery, its provenance, and linkage to prevailing monsoon circulation patterns in the Maldives area since the Late Quaternary.

In addition to the aeolian influx, sea-level fluctuations and bottom currents played a significant role in the evolution of the sedimentary system of the Maldives (Betzler et al., 2009, 2013a, 2016; Lüdmann et al., 2013). Relative sea-level highstands caused a flooding of the carbonate platforms and an export of shallow-water carbonate sediments into the adjacent basins, whereas sea-level lowstands caused an exposure of the platforms and likely a strengthened restriction of the Inner Sea area (Schlager et al., 1994; Paul et al., 2012; Lüdmann et al., 2013; Betzler et al., 2013b, 2016). Moreover, previous studies have shown that during times of restricted water circulation in the Inner Sea the deposition of organic matter was likewise facilitated (Betzler et al., 2016). In recent times, the decay of organic matter in the water column and the generally reduced ventilation of regional subsurface waters in the Indian Ocean results in the development of a strong Oxygen Minimum Zone (OMZ) between 200 and 1200 m water depth (Reid, 2003; Stramma et al., 2008). This oxygen depletion is fostered by the semi-enclosed nature of the northern Indian Ocean, the long pathway of intermediate water from its main formation sites at 40° S in the central South Indian Ocean (Antarctic Intermediate Water, AAIW) and Indonesia (Indonesian Intermediate Water, IIW) (Olson et al., 1993; You, 1998), and the contribution of low-oxygen outflow waters from the Red Sea and the Persian Gulf (Jung et al., 2001; Prasad and Ikeda, 2001). The OMZ extends from the Arabian Sea into the equatorial Indian Ocean. While oxygen concentrations in the Arabian Sea can be as low as 0.1 ml l^{-1} (or 5 µmol kg^{-1}) (Reid, 2003), they still reach low oxic values of around 1 ml l^{-1} (or 45 µmol kg^{-1}) in 500 to 1000 m water depths of the Maldives region (Weiss et al., 1983; Reid, 2003). Phases of an intensified OMZ in the northern Indian Ocean are controlled by both changes in ventilation of intermediate-/deep-water masses (Schmiedl and Leuschner, 2005; Ziegler et al., 2010; Das et al., 2017), and by regional oxygen consumption responding to monsoon-driven upwelling and high surface productivity (e.g. Reichart et al., 1998; Den Dulk et al., 2000; Das et al., 2017). This addresses the ongoing debates, if fluctuations of the OMZ in the Maldives area can be linked to a basin-wide change in the composition of intermediate waters and/or super-regional oceanic processes, respectively. And what is the role of regional sea-level changes in this context.

Here we present a multi-proxy data set on the links between climate variability, ocean circulation, sedimentation and biogeochemical processes of the Maldives Inner Sea. Specifically, our study addresses the following questions: (1) Which impact did orbital-scale changes of the Indian monsoon have on dust fluxes and marine environments of the Maldives? (2) How did global sea-level changes influence the sedimentation processes and benthic ecosystems of the Maldives Inner Sea? (3) Can we trace the influence of changes in the configuration of intermediate waters and how are these changes related to super-regional oceanographic processes? The Maldives Inner Sea is ideally situated to answer these questions because it lies in the central part of the Indian Ocean and is therefore situated in a region influenced the different processes introduced above. The Maldives also appear as an ideal place to trace back paleoceanographic variations in time, as seismic surveys have shown that the Maldives are comparable to a large natural sediment trap with a continuous succession since the Neogene (Betzler et al. 2009, 2013a, 2013b, 2016; Lüdmann et al., 2013).

2 Material and Methods

2.1 Sediment cores and material descriptions

For this study, two sediment cores were retrieved from different sites in the Inner Sea of the Maldives (Fig. 1). The 5.97 m long sediment core SO236-052-4 was obtained by means of a gravity corer in the framework of R/V SONNE cruise SO236 in August 2014, E of the North Ari Atoll in the central part of the Inner Sea (03°55.09'N; 73°08.48'E) and from a water depth of 382 m. The 12.94 m long sediment core M74/4-1143 is a piston core from R/V METEOR cruise M74/4, obtained in 2007 from E of the Goidhoo Atoll (04°49.50'N; 73°05.04'E) at a water depth of 387 m (Fig. 1). For comparison with the gravity core, this study is focused on the first 6.00 m of core M74/4-1143.

The sediment of core SO236-052-4 consists of an alternation of non-lithified fine-grained ooze with abundant pteropods, sponge spicules, planktonic and benthic foraminifera, and echinoid remains, with minor otolites and fragments of gastropods and bivalves. There are locally some intervals that present up to 4 cm bioclast including solitary corals and thin-shelled bivalves. The entire succession is intensely reworked by bioturbation. Just a few primary structures, usually main boundaries between facies are preserved (i.e. the sharp contacts at 2.35 meters below sea-floor, mbsf, and at 3.90 mbsf). Discrete burrows are scarce. The succession recovered at site M74/4-1143 has been described by Betzler et al. (2013b). The core consists mainly of periplatform ooze containing planktonic foraminifera, pteropods, otoliths, mollusc remains, benthic foraminifers, sponge spicules, and echinoid debris. Down the core, light and dark colored greenish to olive gray intervals alternate (Betzler et al., 2013b).

2.2 Geochemical analyses

Scanning X-Ray Fluorescence (XRF) element analysis of core SO236-052-4 was carried out at the MARUM, University of Bremen, using an Avaatech XRF Core Scanner II. Element analysis was performed at 1 cm intervals, using generator settings of 50 kV (1.0 mA current), 30 kV (1.0 mA) and 10 kV (0.2 mA), and a sampling time of 20 seconds per measurement. Raw data spectra were processed using the software package WIN AXIL. Element ratios (Fe/Al, Ti/Al, Si/Ca, Sr/Ca) were calculated and used for environmental interpretations following Martin et al. (1991), Zhang et al. (1993), Boyd et al. (2000), Gao et al. (2001), Lourens et al. (2001), Jickells et al. (2005), Itambi et al. (2009) and Croudace and Rothwell (2015). Bromine (Br) XRF counts were used as indicator of variability in the marine organic carbon (MOC) content (Ziegler et al., 2008; Caley et al., 2013).

The total inorganic carbon (TIC, calcium carbonate) and total organic carbon (TOC) contents of core SO236-052-4 were measured at 5 cm spacing. The carbon content of the grain-size fraction < 63 µm was determined using a LECO DR144 carbon analyser. All samples were freeze-dried. Subsequently, one subsample was measured at 1350 °C to obtain the total carbon (TC) content. A second subsample was heated to 550 °C for 5 hours to remove the organic carbon prior to measurement in the LECO; this gave the TIC content. The difference between TC and TIC contents is regarded as the TOC content. Calcium carbonate contents were then calculated from the total inorganic carbon content as follows: $CaCO_3$ (%) = (TC - TOC) × 8.33, where 8.33 is the atomic proportion of carbon in $CaCO_3$ (e.g. Müller et al., 1994; di Primio and Leythaeuser, 1995; Romero et al., 2006).

2.3 Grain-size analyses

For bulk grain size analysis, core SO236-052-4 was sampled equidistantly (1.5 cm^3 each 1 cm). Samples were wet-sieved (2000 µm) to remove very coarse particles, and subsequently suspended in water with addition of a 0.05 % solution of Tetrasodium Diphosphate Decahydrate as dispersant.

The mean grain size of the non-carbonate fraction between 10 to 63 µm, the sortable silt, has been shown to be a reliable proxy for palaeocurrent strength in predominantly siliciclastic sediments (Manighetti and McCave, 1995; McCave et al., 1995a, 1995b; Hall et al., 1998; Bianchi et al., 1999; McCave and Hall, 2006). The method makes use of the non-carbonate fraction only and is therefore expected to be unaffected by primary carbonate production and burial diagenesis. Samples for the determination of the sortable silt component (c. 20 cm^3 each) were taken equidistantly (in core M74/4-1143 at 5 cm intervals down to 1 m core depth and at 10 cm intervals underneath, and at 5 cm downcore intervals in core SO236-052-4). Subsequently to wet-sieving, the fraction < 63µm was cooked in H_2O_2 to remove the organic portion, and treated with 1M Ca_3COOH to dissolve the carbonate. Biogene opal was removed with 2M $NaHCO_3$. The remainder was dispersed in water for grain-size determination.

Bulk grain size and sortable silt measurements were done using a Helos KF Magic Laser particle size analyzer and measuring ranges of either 0.5/18-3500 µm (for bulk grain size) or 0.25-87.5 µm (for the non-carbonate fraction). To ensure accuracy of measurements and absence of a long-term instrumental drift, an in-house grain-size standard was measured regularly. Grain size statistics are based on the graphical method (Folk and Ward, 1957) and were calculated using the software GRADISTAT (Blott and Pye, 2001).

2.4 Foraminiferal faunal and stabile isotope analyses

For stable isotope analyses core SO236-052-4 was sampled at 5 cm spacing, and for benthic foraminiferal faunal analysis at 10 cm spacing. All samples were wet-sieved over a 63 µm screen and the residues subsequently dried at 38 °C. The benthic foraminiferal analysis was carried out on the > 125 µm size fraction and based on allocate splits in order to obtain approximately 300 tests. Genus and species identifications mainly based on Loeblich and Tappan (1988), Hottinger et al. (1993), Jones (1994), Debenay (2012), Milker and Schmiedl (2012) and Holbourn et al. (2013). The genera *Cymbaloporetta* and *Tretomphaloides* were summarized as meroplanktonic benthic foraminifera (BF) since they are known to have planktonic drift phases as part of their dispersal strategy (Banner et al., 1985; Alve, 1999). For analysis based on the test material all individuals of the foraminiferal orders Astrorhizida, Lituolida and Textulariida were summarized as agglutinated BF.

Benthic foraminiferal assemblages were defined by Q-mode Principal Component Analysis (PCA) with varimax rotation using the software SYSTAT, version 5.2.1. Following Schmiedl et al. (1997), only foraminiferal taxa with percentages ≥ 1 %

in at least one sample and/or taxa, which occur at least in two samples were used for the statistical analysis. Loadings ≥ 0.5 were defined as significant (Backhaus et al., 2008). The Shannon-Wiener diversity index H(S) was calculated after Murray (2006) based on the function H(S) = (-1) $\sum_{i=1}^{S} p_i \times \ln(p_i)$, where S is the species number and p_i the relative abundance of the i-th species.

Stable oxygen and carbon isotope records were generated for planktonic and benthic foraminifera. Approximately 10 tests of the planktonic foraminifer *Globigerinoides ruber* (white) were selected from the 250-350 µm size fraction of core SO236-052-4. Stable isotope data of *G. ruber* (white) of core M74/4-1143 were taken from Betzler et al. (2013b). In addition, approximately 2-5 tests of the epibenthic foraminifera *Cibicides mabahethi* and of the deep infaunal species *Globobulimina affinis* s.l. were selected from the size fraction > 125 µm of core SO236-052-4. Stable oxygen and carbon isotope analyses were performed with Finnigan MAT253 gas mass spectrometer coupled to automatic carbonate preparation device Kiel IV, respectively. The mass spectrometer was calibrated to the PDB scale via international standard NBS19, and results are given in δ-notation versus VPDB. Based on measurements of an internal laboratory standard (Solnhofen limestone) together with samples over a 1-year period, precision was better than 0.08 ‰ for $\delta^{18}O$ and 0.06 ‰ for $\delta^{13}C$, respectively.

For core SO236-052-4 changes in bottom water oxygen concentrations were estimated based on the $\delta^{13}C$ difference between the epifaunal (*C. mabahethi* = *Cm*) and deep infaunal (*G. affinis* s.l. = *Ga*) benthic foraminifera using the function $\Delta\delta^{13}C = 0.00772 \times [O_2] + 0.41446$, wherein $[O_2]$ concentrations between 55 and 235 µmol kg^{-1} have shown a strong linear relationship between bottom water $[O_2]$ and $\Delta\delta^{13}C$ (Hoogakker et al., 2015). We also applied this function to the low $[O_2]$ values ($[O_2]$ < 55 µmol kg^{-1}), because such a relationship may also exist for low $[O_2]$ values and $\Delta\delta^{13}C$, although not investigated by Hoogakker et al. (2015). For $[O_2]$ reconstruction two $\delta^{13}C$ values of core SO236-052-4 (at 0.17 and 130.92 ka) have not been considered due to the weak validity in the $\delta^{13}C_{Ga}$ signal. For comparison, oxygen concentration changes of a deep-sea sediment core from an Arabian Sea site (GeoB3004, 1803 m water depth) were taken from Schmiedl and Mackensen (2006). These data are based on the difference between the epifaunal *Cibicidoides wuellerstorfi* (*Cw*) and *G. affinis* (*Ga*). Further, the $\delta^{13}C$ gradient between *G. ruber* (white; *Gr*) and *C. mabahethi* (*Cm*) of core SO236-052-4 was estimated to assess the sea surface and bottom-water stabile carbon isotope difference and water column mixing.

2.5 Spectral analyses

For the evaluation of periodic temporal variability Blackman-Tukey spectral analyses were performed for TOC, Fe/Al and Ti/Al ratios, Br XRF counts of core SO236-052-4, and the reconstructed oxygen concentrations of core SO236-052-4 and Arabian Sea core GeoB3004 (Schmiedl and Mackensen, 2006), in comparison to the Δ-insolation at 30° N. The analyses were carried out with the AnalySeries software, version 2.0, 05/2005 (Paillard et al., 1996). Prior to the analyses, the records of SO236-052-4 were rescaled with $\Delta t = 2$ ka (TOC, oxygen) and $\Delta t = 0.5$ ka (Fe/Al, Ti/Al, Br XRF counts), and the oxygen record of GeoB3004 with $\Delta t = 1$ ka.

2.6 Radiocarbon dating and compilation of the age model

Accelerator Mass Spectrometry (AMS) radiocarbon dating was carried out at the Beta Analytic Radiocarbon Dating Laboratory on mixed surface-dwelling planktonic foraminifera from 35 cm, 80 cm and 140 cm depth of core SO236-052-4 (Table 1). Due to the contrasting available reservoir age correction values (varying between 301 to 544 years; Dutta et al., 2001; Southon et al., 2002), the AMS ^{14}C ages were corrected for the global reservoir age of 400 years in order to minimize potential errors and converted to calendar years using the radiocarbon calibration program CALIB (version 7.0.4; Stuiver and Reimer, 1993) and the calibration curve Marine13 (Reimer et al., 2013). Additional age tie points were derived from graphical correlation of the benthic $\delta^{18}O$ record of core SO236-052-4 with the LR04 standard benthic stack (Lisiecki and

Raymo, 2005) using the software AnalySeries 2.0 (version 5/2005; Paillard et al., 1996). The age model of core M74/4-1143 (Betzler et al., 2013b) was revised by graphical correlation with the planktonic δ^{18}O record of core SO236-052-4 (Fig. 2).

We will provide all data records of core SO236-052-4, which were used and discussed in this manuscript, to the PANGAEA Open Access library.

3 Results

3.1 Age model and sedimentation rate

Based on the radiocarbon ages and the alignment of the stable oxygen isotope stratigraphy, core SO236-052-4 comprises sediments of the past 207.7 ka, respectively (Fig. 2). The top 6 m of sediment core M74/4-1143 comprise the past 242.3 ka. Average sedimentation rates varied between 3.5 cm ka^{-1} in SO236-052-4 and 4.4 cm ka^{-1} in M74/4-1143. Maximum sedimentation rates occurred during interglacial intervals, with 6.8 cm ka^{-1} (SO236-052-4) and 8.4 cm ka^{-1} (M74/4-1143) for the Eemian, and 7.1 cm ka^{-1} (SO236-052-4) to 3.0 cm ka^{-1} (M74/4-1143) for the Holocene (Fig. 2).

3.2 Foraminiferal stable oxygen and carbon isotope records

The δ^{18}O values of core SO236-052-4 vary between -3.09 and -0.68 ‰ in the planktonic *G. ruber*, between 0.91 and 2.51 ‰ in the epibenthic *C. mabahethi*, and between 1.10 and 5.02 ‰ in the deep infaunal *G. affinis* (Fig. 3). Generally, the δ^{18}O records reveal a consistent picture with relatively higher values during glacial intervals and lower values during interglacial intervals. The δ^{13}C values of core SO236-052-4 vary between 0.12 and 1.25 ‰ in *G. ruber*, between 0.22 and 0.91 ‰ in *C. mabahethi*, and between -0.84 to 0.27 ‰ in *G. affinis* (Fig. 3). Despite considerable short-term variability, all records reveal a stepwise increase of δ^{13}C values with lowest values during the Marine Isotope Stage (MIS) 6 and highest values during the Holocene (Fig. 3).

Considering the past bottom-water oxygen concentration reconstruction for core SO236-052-4 by using the $\Delta\delta^{13}C_{Cm\text{-}Ga}$ estimation, the $[O_2]$ values varied between 10.43 µmol kg^{-1} (≙ 0.50 ‰ $\Delta\delta^{13}C_{Cm\text{-}Ga}$) and 139.45 µmol kg^{-1} (≙ 1.49 ‰ $\Delta\delta^{13}C_{Cm\text{-}Ga}$) with average values of approximately 67.10 µmol kg^{-1} (≙ 0.93 ‰ $\Delta\delta^{13}C_{Cm\text{-}Ga}$). In addition, a long-lasting oxygen depletion was observed, starting from the end of MIS 5 to the end of MIS 3 (duration of ~50 ka), and with average oxygen concentrations of approximately 52.50 µmol kg^{-1}. The oxygen concentration of sediment core GeoB3004 (W Arabian Sea) showed an average oxygen content of approximately 81.75 µmol kg^{-1} (≙ 1.05 ‰ $\Delta\delta^{13}C_{Cw\text{-}Ga}$), with variations between 22.04 µmol kg^{-1} (≙ 0.58 ‰ $\Delta\delta^{13}C_{Cw\text{-}Ga}$) and 133.87 µmol kg^{-1} (≙ 1.45 ‰ $\Delta\delta^{13}C_{Cw\text{-}Ga}$) (Schmiedl and Mackensen, 2006). Spectral analyses of the oxygen records of cores SO236-052-4 and GeoB3004 reveal strong power in the precession band (Fig. 4a). The comparatively long lasting oxygen depletion during the last glacial period at site SO236-052 is not observed at site GeoB3004.

The $\Delta\delta^{13}C_{Gr\text{-}Cm}$ calculation for site SO236-052 showed maximum differences of the planktonic and epibenthic stabile δ^{13}C values (0.68 ‰) during the full interglacial periods of MIS 7, 5 and 1, coinciding with global sea-level highstands. Accordingly, minimum differences (-0.54 ‰) were documented for the glacial periods MIS 6 and 2 and sea-level lowstands.

3.3 Sedimentological and geochemical records

The detailed sedimentological and geochemical data of core SO236-052-4 reveal a glacial-interglacial pattern but also considerable short-term variability (Figs. 4c-f, 5). Sortable silt records are available for both sites and in general they show coarser means during interglacial times, up to 14 µm during the Holocene and > 13 µm during the Eemian (Figs. 5a, 6). However, absolute values and variability are much greater in core M74/4-1143 which is located in the drift of the Kardiva Channel (see: Betzler et al., 2013b) compared to core SO236-052-4 from the more sheltered part of the Inner Sea. In core

M74/4-1143, sortable silt shows an increase towards the MIS 6/5 transition (Termination II) followed by generally elevated values during the Eemian (maximum 27.17 µm), whereas there is much less variability at the same time in the data from core SO236-052-4. Both cores show a coarsening of the sortable silt towards the MIS 1.

Bulk mean grain size shows a pronounced glacial-interglacial variability with up to 57 µm during the MIS 2 and MIS 6 and values between 10 and 30 µm for the remainder (Fig. 5a). Finest sediments occur during the early MIS 5 and the MIS 1 (10 µm).

Total organic carbon (TOC) and calcium carbonate ($CaCO_3$) contents of core SO236-052-4 reveal reverse glacial-interglacial trends with maximum TOC content during glacial- and maximum carbonate contents during interglacial periods. TOC varies between 0.85 wt. % (interglacial) and 2.06 wt. % (glacial), whereas the carbonate content varies between 77.03 wt. % (glacial) and 89.40 wt. % (interglacial) (Fig. 5b).

Both, the Fe/Al and Ti/Al records, show similar patterns with relatively higher values during glacial periods and with slightly increasing values towards today. The Br XRF counts and the Si/Ca ratio show similar distinct glacial-interglacial patterns, comparable to the TOC record, with generally higher values during glacial periods and lower values during interglacial periods (Fig. 5d). Further, the Si/Ca record is characterized by an abrupt and short-lasting maximum at Termination II (Fig. 5d). Inverse patterns are observed for the Sr/Ca record, which follows the inversed $\delta^{18}O$ curve and shows higher values during interglacial and lower values during glacial periods (Fig. 5d).

Spectral analyses of the TOC, Ti/Al and Br reveal significant but considerably weaker variability in the precession band when compared to the reconstructed oxygen records (Fig. 4c, e). The Fe/Al record lacks substantial precessional variability but is rather dominated by long-term glacial-interglacial changes (Fig. 4e).

3.4 Benthic foraminiferal record

In sediment core SO236-052-4, a total of 256 different benthic foraminiferal species were distinguished, with 51 to 93 different species per sample. The diversity H(S) is relatively high and varies between 3.3 and 4.0, with a slight long-term decrease towards today (Fig. 7a). The foraminiferal fauna at the Inner Sea is dominated by hyaline taxa. In comparison, agglutinated individuals were less abundant, but with increasing relative abundances up to approximately ≥ 20 % of the entire fauna during the glacial periods (Fig. 8e). The three-component model of the Q-mode PCA explains 89.14 % of the total variance (Table 2). Assemblage 1 (PC1) explains 31.54 % of the total variance and is dominated by *Neouvigerina proboscidea* and *Discorbinella araucana*, with *Hyalinea inflata*, *Cymbaloporetta squammosa*, *Bulimina marginata* and *Rosalina vilardeboana* as associated taxa (Table 2). This assemblage occurred mainly during the late MIS 7 and 5 and is less pronounced during MIS 4 to early MIS 2 (Fig. 7b). Assemblage 2 (PC2) explains 30.54 % of the total variance and is dominated by *Cibicides mabahethi*, with *Discorbinella bertheloti*, *Siphogenerina columellaris*, *Gyroidina umbonata*, *Reophax* sp., *H. inflata*, and *D. araucana* as associated taxa (Table 2). Assemblage 2 occurred mainly during MIS 6 and 1 (Fig. 7c). Assemblage 3 (PC3) explains 27.06 % of the total variance and is dominated by *N. proboscidea* and *Hoeglundina elegans*, with *D. bertheloti*, *Cibicidoides subhaidingeri*, *Discorbis* sp., *Spiroplectinella sagittula* s.l., and *C. mabahethi* as associated taxa (Table 2). Assemblage 3 occurred during MIS 4 to 2 (Fig. 7d). The distribution of the most important benthic foraminiferal species, which characterize the three faunal assemblages, are displayed in Fig. 7e-g. The most abundant species include *C. mabahethi* (maximum relative abundance of ~17 % during MIS 6), the weakly hispid *N. proboscidea* (maximum of ~16 % at the end of MIS 5) and *D. araucana* (maximum of ~11 % during the onset of MIS 5). Meroplanktonic benthic foraminifera (genera *Cymbaloporetta* and *Tretomphaloides*) occurred in elevated numbers during interglacial periods (maximum of 10.88 %), particularly during MIS 5 (Figs. 6d, 7e).

4 Discussion

4.1 Dust fluxes, marine productivity and monsoon variability

The Ti/Al and Fe/Al in core SO236-052-4 were used as proxies for terrigenous sediment delivery, reflecting changes in the deposition of aeolian dust and thus in the aridity of the hinterland/source area of the dust (Zhang et al., 1993; Lourens et al., 2001; Itambi et al., 2009). Local sources of Fe-rich sediments can be excluded since the sediments of the Maldives archipelago and adjacent shallow- to deep-water environments are characterized by carbonates comprising reef and lagoon carbonates of the islands and pelagic deep-water carbonates (Betzler et al., 2013b; Reolid et al., 2017). This is also reflected by the calcium carbonate content, which is very high at site SO236-052 throughout the past 200 ka (Fig. 5b). Studies on modern aerosols of the North Pacific region indicate that most of the oceanic iron input is derived from atmospheric transport after mobilisation from the central Asian deserts and Chinese loess plateau (Duce and Tindale, 1991). Accordingly, the most likely dust sources for the observed Fe in the sediments of the Maldives are the Indian subcontinent and the Asian desert and loess areas (Roberts et al., 2011), although a minor contribution from northeast Africa and Arabia cannot be excluded (Chauhan and Shukla, 2016). The latter regions rather have been identified as major dust sources in the Arabian Sea based on specific clay mineral composition and magnetic susceptibility of the lithogenic fraction (deMenocal et al., 1991; Sirocko and Lange, 1991). Northwest winds over the Arabian Peninsula blow dust into the Arabian Sea, when the Arabian source areas undergo aridification during high-latitude ice cover (deMenocal et al., 1991; Sirocko and Lange, 1991). In the northwestern Arabian Sea, associated dust fluxes are in phase with maximum ice volume but also vary in the precessional band, suggesting a likewise strengthening of the SW summer monsoon as an important regional driver (Clemens and Prell, 1990; Clemens et al., 1996). In contrast, in the eastern equatorial Indian Ocean the majority of dust is transported via the NE monsoon, coinciding with the prevailing wind system, which blows during northern hemisphere winter. Therefore, elevated Fe/Al and Ti/Al ratios at site SO236-052 indicate the combined effects of enhanced glacial dust availability in the source areas and dust transport to the Maldives with generally strengthened NE monsoon winds during the glacial intervals of MIS 6 and MIS 4-2. On a global scale, the generally colder and drier glacial conditions resulted in a two- to fivefold increase of dust fluxes (Maher et al., 2010).

The observed response of the winter circulation of the Maldives to glacial conditions is in line with the finding of a general strengthening of the NE Indian monsoon after initiation of the northern hemisphere glaciation (Gupta and Thomas, 2003). But our dust proxies show little (Ti/Al) or no (Fe/Al) variability at the precessional band (Fig. 4e), which should be expected if the dust fluxes were directly proportional to the intensity of the winter monsoon (Caley et al., 2011a, b). For a statistically more robust evaluation of the full orbital variability (including the long-wave components) considerably longer time series would be required. Nevertheless, graphical comparison of our data series reveals a dominant eccentricity component in the dust proxies with pronounced glacial-to-interglacial changes, suggesting a link to high-latitude climate and environmental changes (Fig. 8). Therefore the dust records of the Maldives Inner Sea are mainly driven by the generally enhanced dust availability during glacial intervals. As a major dust source, the Chinese loess plateau is strongly influenced by the East Asian Monsoon (EAM). During the Late Quaternary, EAM and related vegetation changes are characterized by predominant eccentricity cycles associated with the advance and retreat of the boreal ice sheets (Ding et al., 1995; Liu et al., 1999; Sun et al., 2006; Hao et al., 2012). Our conclusion is also in line with the lithogenic flux reconstructions from the Arabian Sea (e.g. site ODP722; Clemens et al., 1996), which show striking changes on the glacial-to-interglacial timescale (in the eccentricity band) and suggest a close relation between high-latitude climate and aridity of the dust source areas. On the Chinese loess plateau, the onset of glacial conditions led to an abrupt increase of atmospheric dust loadings (Zhang et al., 2002), suggesting the operation of climate-vegetation feedbacks. Enhanced deposition of terrestrial particles at site SO236-052 led to a generally coarsening of the glacial sediment and fostered the distribution of agglutinated benthic foraminifera, which reached a relative abundance of up to ~20 % during the last glacial period (Figs. 5, 8e). Most agglutinated foraminifera in core SO236-052-4 belong to the Textulariida, such as *Spiroplectammina sagittula*, *Textularia calva* or *Textularia pala*. These and related taxa are often associated with relatively coarse-grained substrates and they preferentially use siliciclastic grains for building up their test walls (Allen et al., 1999; Murray, 2006; Armynot du Châtelet et al., 2013).

The modern equatorial Indian Ocean is limited in the micronutrient iron (Wiggert et al., 2006; Maher et al., 2010) and therefore, enhanced aeolian Fe fluxes to the ocean during glacial periods likely have a direct impact on the seasonal surface productivity (Martin et al., 1991; Boyd et al., 2000; Gao et al., 2001; Jickells et al., 2005), which also influences the deep-sea benthic ecosystems through seasonal phytodetritus pulses. Similar relations between Fe fluxes and surface ocean productivity have been reported from the Southern Ocean (Anderson et al., 2014; Martínez-García et al., 2014) and the equatorial Pacific Ocean (Costa et al., 2016). The TOC and Br contents of marine sediments are widely used as proxies for organic matter fluxes and surface water productivity (Müller and Suess, 1979; Rühlemann et al., 1999; Ziegler et al., 2008 2009; Caley et al., 2013). But the applicability of both proxies in quantitative reconstructions is limited by the specific sedimentological and biogeochemical processes at the sediment-water interface, including the bulk accumulation rate and bottom water oxygenation (Möbius et al., 2011; Schoepfer et al., 2015; Naik et al., 2017). However, elevated TOC and Br values in core SO236-052-4 suggest generally enhanced organic matter fluxes during glacial periods, which may reflect the influence of Fe fertilisation (Fig. 8b-d).

The benthic foraminiferal faunas at site SO236-052 reveal a marked glacial-interglacial pattern (Figs. 7, 8f). The diversity, microhabitat partitioning and species composition of deep-sea benthic foraminiferal faunas is mainly controlled by the combined influences of quantity and quality of food supply and oxygen content of the bottom and pore waters (Jorissen et al., 1995; Fontanier et al., 2002). The diversity of the faunas is high, with H(S) values always > 3.2, throughout the studied time interval, suggesting the absence of extreme environmental conditions at the sea floor of the study site. Therefore, the observed faunal changes likely reflect variations in the amount and quality of food supply. The most abundant species of the three benthic foraminiferal assemblages comprise *C. mabahethi, N. proboscidea* and *D. araucana*, all with PC scores > 3 in at least one assemblage (Table 2). Microhabitat studies demonstrated that most species of the genera *Cibicides* and *Cicididoides* live as suspension feeders on or elevated above the sea floor (Lutze and Thiel, 1989; Linke and Lutze, 1993), therefore we assume a similar microhabitat preference for *C. mabahethi*. In the Red Sea, this species is adapted to relatively high oxygen contents and low organic matter fluxes (Edelman-Furstenberg et al., 2001; Badawi et al., 2005). The cosmopolitan *N. proboscidea* inhabits an epifaunal to very shallow infaunal microhabitat (Fontanier et al., 2002; Licari et al., 2003) and has been described as detritus feeder from various bathyal and abyssal environments. In the South Atlantic Ocean, *N. proboscidea* is associated with well-ventilated and oligotrophic conditions (Schmiedl et al., 1997). Whereas this species thrives under moderate to high organic matter fluxes and oxygen-depleted intermediate waters in the Indian Ocean (Murgese and De Deckker, 2007; De and Gupta, 2010) and was used as a proxy for the strength of the SW monsoon (Gupta and Srinivasan, 1992; Gupta and Thomas, 2003; Sarkar and Gupta, 2014). These observations and the high relative abundance of *N. proboscidea* in core SO236-052-4 during the last glacial intervals MIS 4-2, as well as the interglacial interval MIS 5 suggest an adaptation to a wide range of trophic conditions and confirms its tolerance to moderate oxygen depletion. Little information is available on the ecology of *D. araucana* but its flat trochospiral test morphology and its distribution in the North Atlantic Ocean suggest an epifaunal microhabitat and adaptation to suspended food sources (Corliss and Chen, 1988; Koho et al., 2008). Similar to the closely related *D. bertheloti*, it may prefer oxic conditions (Duleba et al., 1999; Smith and Gallagher, 2003), with a tolerance to moderate oxygen depletion (Edelmann-Furstenberg et al., 2001). The shallow infaunal *Hoeglundina elegans*, which mainly occurs together with *N. proboscidea* in assemblage 3 during MIS 4-2, is commonly associated with low to moderate organic matter fluxes, fresh phytodetritus and high oxygen contents (Corliss, 1985; Koho et al., 2008).

The ecological preferences of the dominant taxa suggest that faunal changes at site SO236-052, although pronounced, were driven by rather subtle changes in the amount of organic matter fluxes. Instead, the faunal changes likely reflect variations in lateral suspension of food particles, substrate-specific development of infaunal niches, and the influence of oxygen changes on the quality of the organic matter. The high dominance of the detritus feeders *N. proboscidea* and *H. elegans* in assemblage 3 reflect highest organic matter fluxes during the last glacial MIS 4-2 (Fig. 8f). In contrast, the dominance of the epifaunal suspension feeder *C. mabahethi* in assemblage 2 during the penultimate glacial (MIS 6) suggests relatively lower organic matter fluxes. The *N. proboscidea/D. araucana* assemblage 1 of MIS 5 reveals some similarity to assemblage 3 but the high abundance of *D. araucana* suggests an overall lower food flux with a considerable amount of suspended particles. In addition, the relatively finer-grained substrate likely opened infaunal niches as indicated by the presence of the shallow to deep infaunal *Bulimina marginata* during the MIS 5 (Jorissen and Wittling, 1999) (Fig. 7e). Contrasts in the boundary conditions between different glacials and interglacials may account for the inconsistent association of certain assemblages to either glacial or interglacial periods. For instance, glacial boundary conditions during MIS 6 were different from MIS 4-2, in which the latter was characterized by relatively higher global ice volume and related lower sea-level (Rohling et al., 2009) and pronounced millennial-scale variability (Dansgaard et al., 1993). Previous studies showed similar patterns, with certain benthic foraminiferal assemblages occurring both during glacial and interglacial periods, e.g. in the Red Sea (Badawi et al., 2005). At the Maldives Inner Sea glacial-to-interglacial changes in food fluxes were likely not extreme and therefore ecological thresholds for certain species and faunas may not have always been passed during glacial-interglacial transitions. A detailed inspection of assemblage 2 (*C. mabahethi*-fauna) actually displays faunal differences between their occurrences in MIS 1 and MIS 6 although *C. mabahethi* is the dominant taxon in both intervals.

While the benthic foraminiferal fauna basically varies on the glacial-interglacial time scale, the TOC, Br and Ti/Al records reveal additional variability in the precessional band (Fig. 4). This suggests that marine environmental conditions in the Maldives are linked to high-latitude climate variability but also to regional monsoonal changes. The surface water productivity of the northern Indian Ocean is driven by wind-induced mixing of the upper water column and upwelling of nutrient-rich subsurface waters and thus reveals a close association with seasonal changes of the monsoonal wind system (Nair et al., 1989). Accordingly, productivity changes in the northern and northwestern Arabian Sea are coherent to the strength of the SW monsoon (Ivanova et al., 2003; Leuschner and Sirocko, 2003; Singh et al., 2011), and along the Indian west coast to the strength of the NE monsoon (Rostek et al., 1997; Singh et al., 2011). The elevated TOC and Br values at site SO236-052 during phases of reduced northern hemisphere summer insolation suggest a direct influence of the Indian winter monsoon on productivity and related organic matter fluxes of the Maldives Inner Sea during the past 200 ka (Fig. 8), which is consistent with the present-day situation (de Vos et al., 2014). The link between the winter monsoon intensity and surface water productivity in the study area is confirmed by the difference between the δ^{13}C values of the epipelagic *G. ruber* and the epibenthic *C. mabahethi* (Fig. 9). Low $\Delta\delta^{13}C_{Gr\text{-}Cm}$ values indicate enhanced vertical mixing of the water column, which is associated with increased supply of nutrients from subsurface waters into the photic zone, based on enhanced surface water productivity.

4.2 Sea-level changes, sedimentation processes and benthic ecosystem dynamics

The close association of changes in sediment composition (i.e. bulk grain size, carbonate content) at site SO236-052 with the LR04 stable benthic isotope stack (Lisiecki and Raymo, 2005) suggests a dominant influence of sea-level changes on the depositional environments of the Maldives Inner Sea. This is also corroborated by the Sr/Ca variations in the core. In periplatform ooze, i.e. areas around shallow water carbonate banks, higher Sr contents are a consequence of higher input of shallow water aragonite (Dunbar and Dickens, 2003), which is produced in the neritic parts of the platforms and exported to the areas around the platform by currents.

As shown by previous studies, variations in the total organic carbon content in the Inner Sea sediments are considerably triggered by sea-level and ocean current changes (Betzler et al., 2016). Thus, the observed changes in bottom currents likely influenced the lateral transport of suspended organic particles as it is suggested by variations in the relative abundance of suspension feeders in the different benthic foraminiferal assemblages (Figs. 7, 8, Table 2). The dominance of *D. araucana* during MIS 5 and *C. mabahethi* during MIS 6 and MIS 1 indicates phases of enhanced lateral food supply, which for the interglacial periods (MIS 5, MIS 1) correlate with reconstructed higher current velocities and sea-level highstands (Fig. 6). This is shown by the higher sortable silt data at site SO236-052, implying higher bottom current velocities, and which is also supported by the higher amplitude of change and the sortable silt values of the drift deposits recovered by core M74/4-1143.

The different sortable silt amplitudes of both settings in the Maldives are due to the restriction of the central part of the Inner Sea (core SO236-052-4), whereas in comparison the deposition area in the Kardiva Channel (core M74/4-1143) is known to be exposed by much stronger current regimes since the Late Pleistocene (Betzler et al., 2013b; Reolid et al., 2017).

The interglacial intervals (mainly MIS 5 and MIS 7, Fig. 6) contain high abundances of meroplanktonic benthic foraminifera (*Cymbaloporetta*, *Tretomphaloides*), which build floating chambers for dispersal (Banner et al., 1985; Alve, 1999). These taxa are commonly found in shelf environments (Milker and Schmiedl, 2012). Their acme during the last interglacial maximum at upper bathyal depth of the Maldives Inner Sea coincides with an almost absence of other displaced species from reef and lagoon environments, such as *Elphidium*, *Amphistegina* or *Operculina* (Parker and Gischler, 2011). This implies a repeated colonization of upper bathyal environments with meroplanktonic taxa from submerged neritic environments during sea-level highstands and conditions of the strengthened bottom water velocity.

4.3 Changes in intermediate water circulation and oxygenation

The epibenthic stable carbon isotope record of core SO236-052-4 lacks a coherent glacial-interglacial pattern but reveals an overall $\delta^{13}C_{Cm}$ increase of ~0.5 ‰ over the past 200 ka (Fig. 10). Long-term trends of similar magnitude have been recorded from sites in the southwestern Pacific Ocean, which were particularly bathed by the well-oxygenated Antarctic Intermediate Water mass (AAIW) during warm intervalls (Thiede et al., 1999; Pahnke and Zahn, 2005; Elmore et al., 2015; Ronge et al., 2015) (Fig. 10). The general resemblance of relative changes in epibenthic $\delta^{13}C$ records from different regions suggests a significant and super-regional role of the AAIW in ventilation of upper bathyal environments of the Maldives Inner Sea, which is consistent with the modern oceanographic situation (You, 1998).

Following the approach of Hoogakker et al. (2015) we estimated the changes in the oxygen content of the intermediate water mass of the Maldives Inner Sea based on the $\Delta\delta^{13}C_{Cm\text{-}Ga}$ signal, i.e. the difference between the $\delta^{13}C$ values of the epifaunal *C. mabahethi* and the deep infaunal *G. affinis* s.l. The resulting $[O_2]$ concentrations display significant power in the precession band (23 ka period), with oxic and low oxic conditions related to northern hemisphere insolation maxima and minima, but they never dropped substantially below 45 µmol kg^{-1} (≈1 ml l^{-1}) (Fig. 9). Moreover, the oxic to low oxic conditions did not seem to pose stress to the benthic foraminiferal fauna. Instead, the proportion of the deep infauna increases exponentially under dysoxic conditions, i.e. at $[O_2]$ values significantly below 1 ml l^{-1} (Jorissen et al., 2007). The lack of dysoxic conditions at site SO236-052 at any time of the past 200 ka is corroborated by the persistent high diversity across glacial and interglacial periods and the low abundance of deep infaunal taxa. However, the reconstructed $[O_2]$ changes in intermediate waters at site SO236-052 resemble those from the deep OMZ of the western Arabian Sea, which is influenced by the advection of oxygen-rich North Atlantic Deep Water (NADW) (Schmiedl and Mackensen, 2006). The dependence of oxygen changes in Indian Ocean water masses from the inflow of Atlantic and Antarctic water masses is corroborated by a number of recent observations from the northwestern and southeastern Arabian Sea (Pattan and Pearce, 2009; Das et al., 2017; Naik et al., 2017). We therefore assume that the OMZ variability in the Maldives Inner Sea is influenced by the overall strength and lateral southward expansion of the Arabian Sea OMZ, by local monsoon-related organic matter fluxes and oxygen consumption, but it is additionally controlled by the ventilation of southern-derived oxygen-rich intermediate waters (AAIW). The ocean-wide linkage of intermediate water ventilation can be assumed, due to the general resemblance of our epibenthic stable carbon isotope record with comparable records from other areas. On the other hand, the significant variability of our new oxygen reconstruction from the Maldives Inner Sea in the precession band and its resemblance with the reconstruction from the Arabian Sea suggests an additional influence of monsoon-driven biogeochemical processes. The resulting changes in the biogeochemical processes at site SO236-052 are illustrated by the establishment and long-term persistence of the benthic foraminiferal assemblage 3 underlining the positive response of *N. proboscidea* and associated species such as *H. elegans* and *D. bertheloti* to moderately reduced oxygen and increased food levels.

The long period of lowered [O_2] values below 60 µmol kg^{-1} centred at MIS 4-3 coincides with a marked monsoon and upwelling maximum in the Arabian Sea (Hermelin and Shimmield, 1995; Clemens and Prell, 2003; Leuschner and Sirocko, 2003; Caley et al., 2011a, b), which caused a strengthening and deepening of the OMZ (Almogi-Labin et al., 2000; Den Dulk et al., 2000; Schmiedl and Leuschner, 2005). The expansion of the Arabian Sea OMZ southward into the equatorial region likely preconditioned the oxygen levels of intermediate waters of the Maldives Inner Sea. There, oxygen minima were further lowered by the reduced glacial advection of the oxygen-rich AAIW and enhanced regional microbial oxygen consumption, reflecting a superposition of high and low-latitude climate signals. Additionally, an abrupt [O_2] drop occur at the end of the last glaciation suggesting a short phase of reduced AAIW advection or increased surface water productivity and related oxygen consumption at depth (Fig. 9).

The present OMZ of the northwestern Indian Ocean extends from the northern Arabian Sea into the tropical Indian Ocean (Reid, 2003), reflecting the reduced ventilation of intermediate water masses (due to its remote position) and the biogeochemical processes related to monsoon-induced organic matter fluxes and microbial oxygen consumption. Indeed, the oxygen concentrations in the Indian Ocean display a gradient with very low values in the northern Arabian Sea and increasing values to the South. This gradient illustrates a clear relation to the monsoon-related biogeochemical processes in the Arabian Sea, but is also a reflection of the remote position of the Arabian Sea in terms of intermediate water ventilation. Nevertheless, a monsoon-induced strengthening of the OMZ in the Arabian Sea (as during MIS 3) will results in an increase of the north-south oxygen gradient in the entire northwestern Indian Ocean, which should then also be detected in the Maldives Inner Sea at a lower amplitude.

Evaluations of calcareous nannoplankton records, used as indicators for surface productivity, from sediment cores of the equatorial Indian and Pacific Ocean reveal significant variability in the precession band and are coherent and in phase with February equatorial insolation (Beaufort et al., 1997, 2001). This orbital pattern suggested a close link of equatorial Indian Ocean productivity to the strength of the Indian Ocean Equatorial Westerlies (IEW) and an ENSO-like forcing of equatorial surface ocean productivity during the Late Quaternary (Beaufort et al., 2001). Accordingly, regional productivity and organic matter fluxes in the wider Maldives area may have also been influenced by changes in the strength of the IEW. However, a strong IEW influence in the Maldives Inner Sea is questioned by the low precessional variability observed in our productivity proxies and the close association of modern phytoplankton blooms of this region with the NE monsoon (Sasamal, 2007; de Vos et al., 2014). To summarize, our new results imply that on orbital time scales changes of the winter monsoon and AAIW advection seem to exert the dominant influence on upper bathyal environments of the Maldives Inner Sea.

5 Conclusions

The integrated evaluation of sedimentological, geochemical and micropaleontological proxy records from the Maldives Inner Sea (tropical Indian Ocean) furthers our understanding of links between equatorial climate variability, sea-level changes, changes in intermediate water ventilation and benthic ecosystem dynamics on orbital time scales during the past 200 ka. The main conclusions are:

(1) Aeolian dust fluxes were considerably enhanced during glacial intervals (MIS 6 and MIS 4-2) as indicated by increased Fe/Al, Ti/Al and Si/Ca ratios, generally coarsening of the bulk sediment, and increased abundance of agglutinated benthic foraminiferal taxa, which use the siliciclastic grains for test formation. The enhanced dust input was linked to phases of generally increased atmospheric dust loads and NE winds, suggesting a close linkage of Maldives marine environments to the aridity of the central Asian loess areas and the strength of the Indian winter monsoon.

(2) Increased vertical mixing during glacial phases of intensified winter monsoon resulted in enhanced surface water productivity and associated organic carbon fluxes to the sea-floor as indicated by TOC values and composition of the benthic foraminiferal fauna. The *Cibicidoides mabahethi* (assemblage 2) and *Neouvigerina proboscidea* (assemblage 3) faunas

dominate during MIS 6 and MIS 4-2 respectively, suggesting differences in the amount and quality of the food delivery for the two glacial intervals. The Br XRF counts and the TOC record reveal additional variability on the precessional band (as shown with the Blackman-Tukey spectral analysis, Fig. 4), which are inversely correlated to northern hemisphere summer insolation underlining a close link of regional vertical mixing of the water column and marine productivity to the Indian winter monsoon.

(3) Glacial-interglacial changes in sea-level controlled the downslope transport of sediment from the Maldives archipelago to the deep-sea environments and influenced the current strength at the benthic boundary layer of the Inner Sea resulting in different grain sizes and substrates. The drift deposits recovered by core M74/4-1143 have shown that highest current intensities occurred during and after the glacial terminations (Fig. 6). Bottom currents in general were stronger during interglacials than during glacials, although core SO236-052-4 show lower current velocities and a lower amplitude of change. Stronger current intensities at the sea floor likely favoured the distribution of certain suspension feeding benthic foraminiferal taxa, such as *D. araucana*.

(4) The long-term trend in the benthic δ^{13}C record mirrors the basin-wide change in the composition of intermediate waters, implying a close linkage to the main formation sites of the AAIW in the Southern Ocean. The precessional changes of estimated oxygen concentrations of intermediate waters are coherent with changes in the deep Arabian Sea. This suggests an influence of the lateral expansion of oxygen minimum waters from the Arabian Sea into the equatorial intermediate Indian Ocean and modulation by inflowing AAIW from the south. The predominance of *N. proboscidea* during a long phase of reduced oxygen concentrations (with average oxygen concentrations around 50 µmol kg^{-1}) during late MIS 5 to late MIS 3 suggests an adaption of this species to the particular biogeochemical conditions and food quality associated with low oxic conditions.

Acknowledgements

We thank the masters and crews as well as the shipboard scientific parties of R/V SONNE SO236 and R/V METEOR M74/4 cruises for their excellent collaboration. Jutta Richarz is thanked for her support during grain size analyses, and Lisa Schönborn and Günther Meyer for technical support during stable isotope measurements. Aurora Elmore and Thomas Ronge are thanked for providing the stabile carbon isotope records of the southwestern Pacific Ocean (cores DSDP593, MD06-2986, MD06-2990/SO136/003) and we thank Yvonne Milker for the many helpful discussions. We acknowledge Luc Beaufort for editorial comments and the two anonymous reviewer, who helped to improve this paper with detailed comments and suggestions considerably. This research used data acquired at the XRF Core Scanner Lab at the MARUM, Center for Marine Environmental Sciences, University of Bremen, Germany. This study was supported by grants 03G0236A of the Federal Ministry of Education and Research. The Ministry of Fisheries and Agriculture of the Maldives is thanked for granting the research permit for Maldivian waters.

References

Allen, K., Roberts, S., and Murray, J. W.: Marginal marine agglutinated foraminifera: affinities for mineral phases, Journal of Micropaleontology, 35, 183–191, doi:10.1144/jm.18.2.183, 1999.

Almogi-Labin, A., Schmiedl, G., Hemleben, C., Siman-Tov, R., Segl, M., and Meischner, D.: The influence of the NE winter monsoon on productivity changes in the Gulf of Aden, NW Arabian Sea, during the last 530 ka as recorded by foraminifera, Marine Micropaleontology, 40, 295–319, doi:10.1016/S0377-8398(00)00043-8, 2000.

Altabet, M. A., Higginson, M. J., and Murray, D. W.: The effect of millennial-scale changes in Arabian Sea denitrification on atmospheric CO_2, Nature, 415, 159–162, doi:10.1038/415159a, 2002.

Alve, E.: Colonization of new habitats by benthic foraminifera: a review, Earth-Science Reviews, 46, 167–185, doi:10.1016/S0012-8252(99)00016-1, 1999.

Anderson, R. F., Barker, S., Fleisher, M., Gersonde, R., Goldstein, S. L., Kuhn, G., Mortyn, P. G., Pahnke, K., and Sachs, J. P.: Biological response to millennial variability of dust and nutrient supply in the Subantarctic South Atlantic Ocean, Philosophical Transactions of the Royal Society A, 372, 1–17, doi:10.1098/rsta.2013.0054, 2014.

Armynot du Châtelet, E., Bout-Roumazeilles, V., Coccioni, R., Frontalini, F., Guillot, F., Kaminski, M. A., Recourt, P., Riboulleau, A., Trentesaux, A., Tribovillard, N., and Ventalon, S.: Environmental control on shell structure and composition of agglutinated foraminifera along a proximal-distal transect in the Marmara Sea, Marine Geology, 335, 114–128, doi:10.1016/j.margeo.2012.10.013, 2013.

Aston, S. R., Chester, R., Johnson, L. R., and Padgham, R. C.: Eolian dust from the lower atmosphere of the eastern Atlantic and Indian Oceans, China Sea and Sea of Japan, Marine Geology, 14, 15–28, doi:10.1016/0025-3227(73)90040-6, 1973.

Backhaus, K., Erichson, B., Plinke, W., and Weiber, R.: Multivariate Analysemethoden, Springer, Berlin, Heidelberg, New York, 1–575, 2008.

Badawi, A., Schmiedl, G., and Hemleben, C.: Impact of late Quaternary environmental changes on deep-sea benthic foraminiferal faunas of the Red Sea, Marine Micropaleontology, 58, 13–30, doi:10.1016/j.marmicro.2005.08.002, 2005.

Banner, F. T., Pereira, C. P. G., and Desai, D.: "Tretomphaloid" float chambers in the Discorbidae and Cymbaloporidae, Journal of Foraminiferal Research, 15, 159–174, doi:10.2113/gsjfr.15.3.159, 1985.

Beaufort, L., Lancelot, Y., Camberlin, P., Cayre, O., Vincent, E., Bassinot, F., and Labeyrie, L.: Insolation cycles as a major control of equatorial Indian Ocean Primary Production, Science, 278, 1451–1454, doi:10.1126/science.278.5342.1451, 1997.

Beaufort, L., de Garidel-Thoron, T., Mix, A. C., and Pisias, N. G.: ENSO-like forcing on oceanic primary production during the Late Pleistocene, Science, 293, 2440–2444, doi:10.1126/science.293.5539.2440, 2001.

Betzler, C., Hübscher, C., Lindhorst, S., Reijmer, J. J. G., Römer, M., Droxler, A. W., Fürstenau, J., Lüdmann, T.: Monsoonal-induced partial carbonate platform drowning (Maldives, Indian Ocean), Geology, 37, 867–870, doi:10.1130/G25702A.1, 2009.

Betzler, C., Fürstenau, J., Lüdmann, T., Hübscher, C., Lindhorst, S., Paul, A., Reijmer, J. J. G., and Droxler, A. W.: Sea-level and ocean-current control on carbonate-platform growth, Maldives, Indian Ocean, Basin Research, 25, 172–196, doi:10.1111/j.1365-2117.2012.00554.x, 2013a.

Betzler, C., Lüdmann, T., Hübscher, C., and Fürstenau, J.: Current and sea-level signals in periplatform ooze (Neogene, Maldives, Indian Ocean), Sedimentary Geology, 290, 126–137, doi:10.1016/j.sedgeo.2013.03.011, 2013b.

Betzler, C., Eberli, G. P., Kroon, D., Wright, J. D., Swart, P. K., Nath, B. N., Alvarez-Zarikian, C. A., Alonso-García, M., Bialik, O. M., Blättler, C. L., Guo, J. A., Haffen, S., Horozal, S., Inoue, M., Jovane, L., Lanci, L. Laya, J. C., Mee, A. L. H., Lüdmann, T., Nakakuni, M., Niino, K., Petruny, L. M., Pratiwi, S. D., Reijmer, J. J. G., Reolid, J., Slagle, A. L., Sloss, C. R., Su, X., Yao, Z., and Young, J. R.: The abrupt onset of the modern South Asian Monsoon winds, Scientific Reports, 6, 29838, doi:10.1038/srep29838, 2016.

Bianchi, G. G., Hall, I. R., McCave I. N., and Joseph, L.: Measurement of the sortable silt current speed proxy using the Sedigraph 5100 and Coulter Multisizer IIe: Precision and accuracy, Sedimentology, 46, 1001–1014, doi:10.1046/j.1365-3091.1999.00256.x, 1999.

Blott, S. J. and Pye, K.: GRADISTAT: a grain size distribution and statistics package for the analysis of unconsolidated sediments, Earth Surface Processes and Landforms, 26, 1237–1248, doi:10.1002/esp.261, 2001.

Böning, P. and Bard, E.: Millennial/centennial-scale thermocline ventilation changes in the Indian Ocean as reflected by aragonite preservation and geochemical variations in Arabian Sea sediments, Geochimica et Cosmochimica Acta, 73, 6771–6788, doi:10.1016/j.gca.2009.08.028, 2009.

Boyd, P. W., Watson, A. J., Law, C. S., Abraham, E. R., Trull, T., Murdoch, R., Bakker, D. C. E., Bowie, A. R., Buesseler, K. O., Chang, H., Charette, M., Croot, P., Downing, K., Frew, R., Gall, M., Hadfield, M., Hall., J., Harvey, M., Jameson, G., LaRoche, J., Liddicoat, M., Ling, R., Maldonado, M. T., McKay, R. M., Nodder, S., Pickmere, S., Pridmore, R., Rintoul, S., Safi, K., Sutton, P., Strzepek, R., Tanneberger, K., Turner, S., Waite, A., and Zeldis, J.: A mesoscale phytoplankton bloom in the polar Southern Ocean simulated by iron fertilization, Nature, 407, 695–702, doi:10.1038/35037500, 2000.

Caley, T., Malaizé, B., Zaragosi, S., Rossignol, L., Bourget, J., Eynaud, F., Martinez, P., Giraudeau, J., Charlier, K., and Ellouz-Zimmermann, N.: New Arabian Sea records help decipher orbital timing of Indo-Asian monsoon, Earth and Planetary Science Letters, 308, 433–444, doi:10.1016/j.epsl.2011.06.019, 2011a.

Caley, T., Malaizé, B., Revel, M., Ducassou, E., Wainer, K., Ibrahim, M., Shoeaib, D., Migeon, S., and Marieu, V.: Orbital timing of the Indian, East Asian and African boreal monsoons and the concept of a ‘global monsoon’, Quaternary Science Reviews, 30, 3705–3715, doi:10.1016/j.quascirev.2011.09.015, 2011b.

Caley, T., Zaragosi, S., Bourget, J., Martinez, P., Malaizé, B., Eynaud, F., Rossignol, L., Garlan, T., and Ellouz-Zimmermann, N.: Southern Hemisphere imprint for Indo-Asian summer monsoons during the last glacial period as revealed by Arabian Sea productivity records, Biogeosciences, 10, 7347–7359, doi:10.5194/bg-10-7347-2013, 2013.

Chauhan, O. S. and Shukla, A. S.: Evaluation of the influence of monsoon climatology on dispersal and sequestration of continental flux over the southeastern Arabian Sea, Marine Geology, 371, 44–56, doi:10.1016/j.margeo.2015.10.018, 2016.

Clemens, S. C. and Prell, W. L.: Late Pleistocene variability of Arabian Sea summer monsoon winds and continental aridity: Eolian records from the lithogenic component of deep-sea sediments, Paleoceanography, 5, 109–145, doi:10.1029/PA005i002p00109, 1990.

Clemens, S. C. and Prell, W. L.: A 350,000 year summer-monsoon multi-proxy stack from the Owen Ridge, Northern Arabian Sea, Marine Geology, 201, 35–51, doi:10.1016/S0025-3227(03)00207-X, 2003.

Clemens, S. C., Prell, W. L., Murray, D. W., Shimmield, G., and Weedon, G.: Forcing mechanisms of the Indian Ocean monsoon, Nature, 353, 720–725, 1991.

Clemens, S. C., Murray, D. W., and Prell, W. L.: Nonstationary Phase of the Plio-Pleistocene Asian Monsoon, Science, 274, 943–948, 1996.

Corliss, B. H.: Microhabitats of benthic foraminifera within deep-sea sediments, Nature, 314, 435–438, doi:10.1038/314435a0, 1985.

Corliss, B. H. and Chen, C.: Morphotype patterns of Norwegian Sea deep-sea benthic foraminifera and ecological implications, Geology, 16, 716–719, doi:10.1130/0091-7613(1988), 1988.

Costa, K. M., McManus, J. F., Anderson, R. F., Ren, H., Sigman, D. M., Winckler, G., Fleisher, M. Q., Marcantonio, F., and Ravelo, A. C.: No iron fertilization in the equatorial Pacific Ocean during the last ice age, Nature, 529, 519–522, doi:10.1038/nature16453, 2016.

Croudace, I. W. and Rothwell, R. G.: Micro-XRF Studies of Sediment Cores: Applications of a non-destructive tool for the environmental sciences, Springer, 1-656, 2015.

Dansgaard, W., Johnsen, S. J., Clausen, H. B., Dahl-Jensen, D., Gundestrup, N. S., Hammer, C. U., Hvidberg, C. S., Steffensen, J. P., Sveinbjörnsdottir, A. E., Jouzel, J., and Bond, G.: Evidence for general instability of past climate from a 250-kyr ice-core record, Nature, 364, 218–220, doi:10.1038/364218a0, 1993.

Das, M., Singh, R. K., Gupta, A. K., and Bhaumik, A. K.: Holocene strengthening of the oxygen minimum zone in the northwestern Arabian Sea linked to changes in intermediate water circulation or Indian monsoon intensity? Palaeogeography, Palaeoclimatology, Palaeoecology, doi:10.1016/j.palaeo.2016.10.035, in press 2017.

De, S. and Gupta, A. K.: Deep-sea faunal provinces and their inferred environments in the Indian Ocean based on distribution of Recent benthic foraminifera, Palaeogeography, Palaeoclimatology, Palaeoecology, 291, 429–442, doi:10.1016/j.palaeo.2010.03.012, 2010.

Debenay, J.-P.: A Guide to 1,000 Foraminifera from Southwestern Pacific, New Caledonia, IRD Éditions, Publications Scientifiques du Muséum, 1–384, 2012.

deMenocal, P. B., Bloemendal, J., and King, J.: A rock-magnetic record of monsoonal dust deposition to the Arabian Sea: Evidence for a shift in the mode of deposition at 2.4 Ma, Proceedings of the Ocean Drilling Program, Scientific Results, 117, 389–407, 1991.

Den Dulk, M., Reichart, G. J., van Heyst, S., Zachariasse, W. J., and Van der Zwaan, G. J.: Benthic foraminifera as proxies of organic matter flux and bottom water oxygenation? A case history from the northern Arabian Sea, Palaeogeography, Palaeoclimatology, Palaeoecology, 161, 337–359, doi:10.1016/S0031-0182(00)00074-2, 2000.

Deplazes, G., Lückge, A., Peterson, L. C., Timmermann, A., Hamann, Y., Hughen, K. A., Röhl, U., Laj, C., Cane, M. A., Sigman, D. M., and Haug, G. H.: Links between tropical rainfall, and North Atlantic climate during the last glacial period, Nature Geoscience, 6, 213–217, doi:10.1038/NGEO1712, 2013.

de Vos, A., Pattiaratchi, C .B., and Wijeratne, E. M. S.: Surface circulation and upwelling patterns around Sri Lanka, Biogeosciences, 11, 5909–5930, doi:10.5194/bg-11-5909-2014, 2014.

di Primio, R. and Leythaeuser, D.: Quantification of the effect of carbonate redistribution by pressure solution in organic-rich carbonates, Marine and Petroleum geology, 12, 735–739, doi:10.1016/0264-8172(95)93598-X, 1995.

Ding, Z., Liu, T., Rutter, N. W., Yu, Z., Guo, Z., and Zhu, R.: Ice-Volume Forcing of East Asian Winter Monsoon Variations in the Past 800,000 Years, Quaternary Research, 44, 149–159, doi:10.1006/qres.1995.1059, 1995.

Duce, R. A. and Tindale, N. W.: Atmospheric transport of iron and its deposition in the ocean, Limnology and Oceanography, 36, 1715–1726, doi:10.4319/lo.1991.36.8.1715, 1991.

Duleba, W., Debenay, J.-P., Eichler, B. B., and de Mahiques, M. M.: Holocene Environmental and Water Circulation Changes: Foraminifer Morphogroups Evidence in Flamengo Bay, (SP, Brazil), Journal of Coastal Research, 15, 554–571, 1999.

Dunbar, G. B. and Dickens, G. R.: Late Quaternary shedding of shallow-water marine carbonate along a tropical mixed siliciclastic-carbonate shelf: Great Barrier Reef, Australia, Sedimentology, 50, 1061–1077, doi:10.1046/j.1365-3091.2003.00593.x, 2003.

Dutta, K., Bhushan, R., and Somayajulu, B. L. K.: ΔR Correction Values for the Northern Indian Ocean, Radiocarbon, 43, 483–488, doi:10.1017/S0033822200038376, 2001.

Edelmann-Furstenberg, Y., Scherbacher, M., Hemleben, C., and Almogi-Labin, A.: Deep-sea benthic foraminifera from the central Red Sea, Journal of Foraminiferal Research, 31, 48–59, 2001.

Elmore, A. C., McClymont, E. L., Elderfield, H., Kender, S., Cook, M. R., Leng, M. J., Greaves, M., and Misra, S.: Antarctic Intermediate Water properties since 400 ka recorded in infaunal (*Uvigerina peregrina*) and epifaunal (*Planulina wuellerstorfi*) benthic foraminifera, Earth and Planetary Science Letters, 428, 193–203, doi:10.1016/j.epsl.2015.07.013, 2015.

Folk, R. L. and Ward, W. C.: Brazos River Bar: A Study in the Significance of Grain Size Parameters, Journal of Sedimentary Petrology, 27, 3–26, 1957.

Fontanier, C., Jorissen, F. J., Licari, L., Alexandre, A., Anschutz, P., and Carbonel, P.: Live benthic foraminiferal faunas from the Bay of Biscay: faunal density, composition, and microhabitats, Deep-Sea Research I, 49, 751–785, doi:10.1016/S0967-0637(01)00078-4, 2002.

Gao, Y., Kaufman, Y. J., Tanré, D., Kolber, D., and Falkowski, P. G.: Seasonal Distribution of Aeolian Iron Fluxes to the Global Ocean, Geophysical Research Letters, 28, 29–32, 2001.

Grand, M. M., Measures, C. I., Hatta, M., Hiscock, W. T., Buck, C. S., and Landing, W. M.: Dust deposition in the eastern Indian Ocean: The ocean perspective from Antarctica to the Bay of Bengal, Global Biogeochemical Cycles, 29, 357–374, doi:10.1002/2014GB004898, 2015.

Guo, Z. T., Ruddiman, W. F., Hao, Q. Z., Wu, H. B., Qiao, Y. S., Zhu, R. X., Peng, S. Z., Wei, J. J., Yuan, B. Y., and Liu, T. S.: Onset of Asian desertification by 22 Myr ago inferred from loess deposits in China, Nature, 416, 159–163, doi:10.1038/416159a, 2002.

Gupta, A. K. and Srinivasan, M. S.: *Uvigerina proboscidea* abundances and paleoceanography of the northern Indian Ocean DSDP Site 214 during the Late Neogene, Marine Micropaleontology, 19, 355–367, doi:10.1016/0377-8398(92)90038-L, 1992.

Gupta, A. K. and Thomas, E.: Initiation of Northern Hemisphere glaciation and strengthening of the northeast Indian monsoon: Ocean Drilling Program Site 758, eastern equatorial Indian Ocean, Geology, 31, 47–50, doi:10.1130/0091-7613(2003), 2003.

Gupta, A. K., Anderson, D. M., and Overpeck, J. T.: Abrupt changes in the Asian southwest monsoon during the Holocene and their links to the North Atlantic Ocean, Nature, 421, 354–357, doi:10.1038/nature01340, 2003.

Hall, I. R., McCave, I. N., Chapman, M. R., and Shackleton, N. J.: Coherent deep flow variation in the Iceland and American basins during the last interglacial, Earth and Planetary Science Letters, 164, 15–21, doi:10.1016/S0012-821X(98)00209-X, 1998.

Hao, Q., Wang, L., Oldfield, F., Peng, S., Qin, L., Song, Y., Xu, B., Qiao, Y., Bloemendal, J., and Guo, Z.: Delayed build-up of Arctic ice sheets during 400,000-year minima in insolation variability, Nature, 490, 393–396, doi:10.1038/nature11493, 2012.

Harrison, T. M., Copeland, P., Kidd, W. S. F., and Yin, A.: Raising Tibet, Science, 255, 1663–1670, 1992.

Hastenrath, S., Nicklis, A., and Greischar, L.: Atmospheric-hydrospheric mechanisms of climate anomalies in the western equatorial Indian Ocean, Journal of Geophysical Research, 98, 20219-20235, doi: 10.1029/93JC02330, 1993.

Hermelin, J. O. R. and Shimmield, G. B.: Impact of productivity events on the benthic foraminiferal fauna in the Arabian Sea over the last 150,000 years, Paleoceanography, 10, 85–116, doi:10.1029/94PA02514, 1995.

Holbourn, A., Henderson, A. S., and MacLeod, N.: Atlas of Benthic Foraminifera, Wiley-Blackwell, Natural History Museum, 1–642, 2013.

Hoogakker, B. A. A., Elderfield, H., Schmiedl, G., McCave, I. N., and Rickaby, R. E. M.: Glacial-interglacial changes in bottom-water oxygen content on the Portuguese margin, Nature Geoscience, 8, 40–43, doi:10.1038/ngeo2317, 2015.

Hottinger, L., Halicz, E., and Reiss, Z.: Recent Foraminiferida from the Gulf of Aqaba, Red Sea, Ljubljana, Slovenska Akademija Znanosti in Umetnosti, 1–179, 1993.

Itambi, A. C., von Dobeneck, T., Mulitza, S., Bickert, T., and Heslop, D.: Millennial-scale northwest African droughts related to Heinrich events and Dansgaard-Oeschger cycles: Evidence in marine sediments from offshore Senegal, Paleoceanography, 24, PA1205, 1–16, doi:10.1029/2007PA001570, 2009.

Ivanova, E., Schiebel, R., Singh, A. D., Schmiedl, G., Niebler, H.-S., and Hemleben, C.: Primary production in the Arabian Sea during the last 135000 years, Palaeogeography, Palaeoclimatology, Palaeoecology, 197, 61–82, doi:10.1016/S0031-0182(03)00386-9, 2003.

Jickells, T. D., An, Z. S., Andersen, K. K., Baker, A. R., Bergametti, G., Brooks, N., Cao, J. J., Boyd, P. W., Duce, R. A., Hunter, K. A., Kawahata, H., Kubilay, N., LaRoche, J., Liss, P. S., Mahowald, N., Prospero, J. M., Ridgwell, A. J., Tegen, I., and Torres, R.: Global Iron Connections Between Desert Dust, Ocean Biogeochemistry, and Climate, Science, 308, 67–71, doi:10.1126/science.1105959, 2005.

Jones, R. W.: The Challenger Foraminifera, The Natural History Museum, London, Oxford University Press, 1–290, 1994.

Jorissen, F. J. and Wittling, I.: Ecological evidence from live-dead comparisons of benthic foraminiferal faunas off Cape Blanc (Northwest Africa), Palaeogeography, Palaeoclimatology, Palaeoecology, 149, 151–170, doi:10.1016/S0031-0182(98)00198-9, 1999.

Jorissen, F. J., de Stigter, H. C., and Widmark, J. G. V.: A conceptual model explaining benthic foraminiferal microhabitats, Marine Micropaleontology, 26, 3–15, doi:10.1016/0377-8398(95)00047-X, 1995.

Jorissen, F.J., Fontanier, C. and Thomas, E.,: Paleoceanographical proxies based on deep-sea benthic foraminiferal assemblage characteristics. In: Hillaire-Marcel, C. and De Vernal, A. (Eds.), Proxies in Late Cenozoic paleoceanography, Developments in Marine Geology, Elsevier, Amsterdam, 277–328, 2007.

Jung, S. J. A., Ganssen, G. M., and Davies, G. R.: Multidecadal variations in the early Holocene outflow of Red Sea Water into the Arabian Sea, Paleoceanography, 16, 658–668, doi:10.1029/2000PA000592, 2001.

Koho, K. A., García, R., de Stigter, H. C., Epping, E., Koning, E., Kouwenhoven, T. J., and Van der Zwaan, G. J.: Sedimentary labile organic carbon and pore water redox control on species distribution of benthic foraminifera: A case study from Lisbon–Setúbal Canyon (southern Portugal), Progress in Oceanography, 79, 55–82, doi:10.1016/j.pocean.2008.07.004, 2008.

Laskar, J., Robutel, P., Joutel, F., Gastineau, M., Correia, A. C. M., and Levrard, B.: A long term numerical solution for the insolation quantities of the Earth, Astronomy & Astrophysics, 428, 261–285, doi: 10.1051/0004-6361:20041335, 2004.

Leuschner, D. C. and Sirocko, F.: Orbital insolation forcing of the Indian Monsoon - a motor for global climate changes? Palaeogeography, Palaeoclimatology, Palaeoecology, 197, 83–95, doi:10.1016/S0031-0182(03)00387-0, 2003.

Licari, L. N., Schumacher, S., Wenzhöfer, F., Zabel, M., and Mackensen, A.: Communities and microhabitats of living benthic foraminifera from the tropical East Atlantic: Impact of different productivity regimes, Journal of Foraminiferal Research, 33, 10–31, doi:10.2113/0330010, 2003.

Linke, P. and Lutze, G. F.: Microhabitat preferences of benthic foraminifera-a static concept or a dynamic adaptation to optimize food acquisition? Marine Micropaleontology, 20, 215–234, doi:10.1016/0377-8398(93)90034-U, 1993.

Lisiecki, L. E. and Raymo, M. E.: A Pliocene-Pleistocene stack of 57 globally distributed benthic δ^{18}O records, Paleoceanography, 20, PA1003, 1–17, doi:10.1029/2004PA001071, 2005.

Liu, T., Ding, Z., and Rutter, N.: Comparison of Milankovitch periods between continental loess and deep sea records over the last 2.5 Ma, Quaternary Science Reviews, 18, 1205–1212, doi:10.1016/S0277-3791(98)00110-3, 1999.

Loeblich, A. R. and Tappan, H.: Foraminiferal Genera and their Classification, Van Nostrand Reinhold Company, New York, 1–2115, 1988.

Lourens, L. J., Wehausen, R., and Brumsack, H.-J.: Geological constraints on tidal dissipation and dynamical ellipticity of the Earth over the past three million years, Nature, 409, 1029–1033, doi:10.1038/35059062, 2001.

Lüdmann, T., Kalvelage, C., Betzler, C., Fürstenau, J., and Hübscher, C.: The Maldives, a giant isolated carbonate platform dominated by bottom currents, Marine and Petroleum Geology, 43, 326–340, doi:10.1016/j.marpetgeo.2013.01.004, 2013.

Lutze, G . F. and Thiel, H.: Epibenthic foraminifera from elevated microhabitats: *Cibicidoides wuellerstorfi* and *Planulina ariminensis*, Journal of Foraminiferal Research, 19, 153–158, doi:10.2113/gsjfr.19.2.153, 1989.

Maher, B. A., Prospero, J. M., Mackie, D., Gaiero, D., Hesse, P. P., and Balkanski, Y.: Global connections between aeolian dust, climate and ocean biogeochemistry at the present day and at the last glacial maximum, Earth-Science Reviews, 99, 61–97, doi:10.1016/j.earscirev.2009.12.001, 2010.

Manabe, S. and Broccoli, A. J.: Mountains and Arid Climates of Middle Latitudes, Science, 247, 192–195, 1990.

Manighetti, B. and McCave, I. N.: Late glacial and Holocene palaeocurrents through South Rockall Gap, NE Atlantic Ocean, Paleoceanography, 10, 611–626, 1995.

Martin, J. H., Gordon, R. M., and Fitzwater, S. E.: The case for iron, Limnology and Oceanography, 36, 1793–1802, 1991.

Martínez-García, A. Sigman, D. M., Ren, H., Anderson, R. F., Straub, M., Hodell, D. A., Jaccard, S. L., Eglinton, T. I., and Haug, G. H.: Iron fertilization of the Subantarctic Ocean during the Last Ice Age, Science, 343, 1347–1350, doi:10.1126/science.1246848, 2014.

McCave, I. N. and Hall, I. R.: Size sorting in marine muds: Processes, pitfalls, and prospects for paleoflow-speed proxies, Geochemistry, Geophysics, Geosystems, 7, 1–37, doi:10.1029/2006GC001284, 2006.

McCave, I. N., Manighetti, B., and Beveridge, N. A. S.: Circulation in the glacial North Atlantic inferred from grain-size measurements, Nature, 374, 149–152, doi:10.1038/374149a0, 1995a.

McCave, I. N., Manighetti, B., and Robinson, S. G.: Sortable silt and fine sediment size/composition slicing: Parameters for palaeocurrent speed and palaeoceanography, Paleoceanography, 10, 593–610, doi:10.1029/94PA03039, 1995b.

Milker, Y. and Schmiedl, G.: A taxonomic guide to modern benthic shelf foraminifera of the western Mediterranean Sea, Palaeontologia Electronica, 15, 16A, 1–134, 2012.

Möbius, J., Gaye, B., Lahajnar, N., Bahlmann, E., and Emeis, K.-C.: Influence of diagenesis on sedimentary δ^{15}N in the Arabian Sea over the last 130 ka, Marine Geology, 284, 127–138, doi:10.1016/j.margeo.2011.03.013, 2011.

Müller, P. J. and Suess, E.: Productivity, sedimentation rate, and sedimentary organic matter in the oceans - I. Organic carbon preservation, Deep-Sea Research, 26, 1347–1362, doi:10.1016/0198-0149(79)90003-7, 1979.

Müller, P. J., Schneider, R., and Ruhland, G.: Late Quaternary $p\mathrm{CO}_2$ variations in the Angola Current: Evidence from organic carbon δ^{13}C and alkenone temperature. In: Zahn, R., Pedersen, T. F., Kaminski, M. A., and Labeyrie, L. (Eds.), Carbon Cycling in the Glacial Ocean: Constraints on the Ocean's Role in Global Change, NATO ASI Series I, Global Environmental Change, 17, Springer-Verlag, Berlin, 343–366, 1994.

Murgese, D. S. and De Deckker, P.: The Late Quaternary evolution of water masses in the eastern Indian Ocean between Australia and Indonesia, based on benthic foraminifera faunal and carbon isotopes analyses, Palaeogeography, Palaeoclimatology, Palaeoecology, 247, 382–401, doi:10.1016/j.palaeo.2006.11.002, 2007.

Murray, J. W.: Ecology and Applications of Benthic Foraminifera, Cambridge University Press, 1–426, 2006.

Naik, D. K., Saraswat, R., Lea, D. W., Kurtarkar, S. R., and Mackensen, A.: Last glacial-interglacial productivity and associated changes in the eastern Arabian Sea, Palaeogeography, Palaeoclimatology, Palaeoecology, doi:10.1016/j.palaeo.2016.07.014, in press 2017.

Nair, R. R., Ittekkot, V., Manganini, S. J., Ramaswamy, V., Haake, B., Degens, E. T., Desai, B. N., and Honjo, S.: Increased particle flux to the deep ocean related to monsoons, Nature, 338, 749–751, doi:10.1038/338749a0, 1989.

NASA Goddard Space Flight Center, Ocean Ecology Laboratory, Ocean Biology Processing Group: MODIS-Aqua Ocean Color Data, doi:10.5067/AQUA/MODIS_OC.2014.0., 2014.

Olson, D. B., Hitchcock, G. L., Fine, R. A., and Warren, B. A.: Maintenance of the low-oxygen layer in the central Arabian Sea, Deep-Sea Research II, 40, 673–685, doi:10.1016/0967-0645(93)90051-N, 1993.

Pahnke, K. and Zahn, R.: Southern hemisphere water mass conversion with North Atlantic climate variability, Science, 307, 1741–1746, doi:10.1126/science.1102163, 2005.

Paillard, D., Labeyrie, L., and Yiou, P.: Macintosh Program Performs Time-Series Analysis, Eos Transactions AGU, 77, 379–379, doi:10.1029/96EO00259, 1996.

Parker, J. H. and Gischler, E.: Modern foraminiferal distribution and diversity in two atolls from the Maldives, Indian Ocean, Marine Micropaleontology, 78, 30–49, doi:10.1016/j.marmicro.2010.09.007, 2011.

Pattan, J. N. and Pearce, N. J. G.: Bottom water oxygenation history in southeastern Arabian Sea during the past 140 ka: Results from redox-sensitive elements, Palaeogeography, Palaeoclimatology, Palaeoecology, 280, 396–405, doi:10.1016/j.palaeo.2009.06.027, 2009.

Paul, A., Reijmer, J. J., Fürstenau, J., Kinkel, H., and Betzler, C.: Relationship between Late Pleistocene sea-level variations, carbonate platform morphology and aragonit production (Maldives, Indian Ocean), Sedimentology, 59, 1640–1658, doi: 10.1111/j.1365-3091.2011.01319.x, 2012.

Pichevin, L., Bard, E., Martinez, P., and Billy, I.: Evidence of ventilation changes in the Arabian Sea during the late Quaternary: Implication for denitrification and nitrous oxide emission, Global Biogeochemical Cycles, 21, GB4008, 1–12, doi:10.1029/2006GB002852, 2007.

Prasad, T. G. and Ikeda, M.: Seasonal spreading of the Persian Gulf Water mass in the Arabian Sea, Journal of Geophysical Research, 106, 17.059–17.071, doi:10.1029/2000JC000480, 2001.

Reichart, G. J., Lourens, L. J., and Zachariasse, W. J.: Temporal variability in the northern Arabian Sea Oxygen Minimum Zone (OMZ) during the last 225,000 years, Paleoceanography, 13, 607–621, doi:10.1029/98PA02203, 1998.

Reid, J. L.: On the total geostrophic circulation of the Indian Ocean: flow patterns, tracers, and transports, Progress in Oceanography, 56, 137–186, doi:10.1016/S0079-6611(02)00141-6, 2003.

Reimer, P. J., Bard, E., Bayliss, A., Beck, J. W., Blackwell, P. G., Ramsey, C. B., Buck, C. E., Cheng, H., Edwards, R. L., Friedrich, M., Grootes, P. M., Guilderson, T. P., Haflidason, H., Hajdas, I., Hatté, C., Heaton, T. J., Hoffmann, D. L., Hogg, A. G., Hughen, K. A., Kaiser, K. F., Kromer, B., Manning, S. W., Niu, M., Reimer, R. W., Richards, D. A., Scott, E. M., Southon, J. R., Staff, R. A., Turney, C. S. M., van der Plicht, J.: IntCal13 and Marine13 Radiocarbon Age Calibration Curves 0-50,000 years cal BP, Radiocarbon, 55, 1869–1887, doi: 10.2458/azu_js_rc.55.16947, 2013.

Reolid, J., Reolid, M., Betzler, C., Lindhorst, S., Wiesner, M. G., and Lahajnar, N.: Upper Pleistocene cold-water corals from the Inner Sea of the Maldives: taphonomy and environment, Facies, 63:8, doi:10.1007/s10347-016-0491-7, 1–20, 2017.

Rixen, T., Haake, B., Ittekkot, V., Guptha, M. V. S., Nair, R. R., and Schlüssel, P.: Coupling between SW monsoon-related surface and deep ocean processes as discerned from continous particle flux measurements and correlated satellite data, Journal of Geophysical Research, 101, 28569–28582, doi:10.1029/96JC02420, 1996.

Roberts, A. P., Rohling, E. J., Grant, K. M., Larrasoaña, J. C., and Liu, Q.: Atmospheric dust variability from Arabia and China over the last 500,000 years, Quaternary Science Reviews, 30: 3537–3541, doi:10.1016/j.quascirev.2011.09.007, 2011.

Rohling, E. J., Grant, K., Bolshaw, M., Roberst, A. P., Siddall, M., Hemleben, C., Kucera, M.: Antarctic temperature and global sea level closely coupled over the past five glacial cycles, Nature Geoscience, 2, 500–504, doi:10.1038/NGEO557, 2009.

Romero, O. E., Kim, J.-H., and Hebbeln, D.: Paleoproductivity evolution off central Chile from the Last Glacial Maximum to the Early Holocene, Quaternary Research, 65, 519–525, doi:10.1016/j.yqres.2005.07.003, 2006.

Ronge, T. A., Steph, S., Tiedemann, R., Prange, M., Merkel, U., Nürnberg, D., and Kuhn, G.: Pushing the boundaries: Glacial/interglacial variability of intermediate and deep waters in the southwest Pacific over the last 350,000 years, Paleoceanography, 30, 23–38, doi:10.1002/2014PA002727, 2015.

Rostek, F., Bard, E., Beaufort, L., Sonzogni, C., and Ganssen, G.: Sea surface temperature and productivity records for the past 240 ka in the Arabian Sea, Deep-Sea Research II, 44, 1461–1480, doi:10.1016/S0967-0645(97)00008-8, 1997.

Ruddiman, W. F. and Kutzbach, J. E.: Forcing of late Cenozoic northern hemisphere climate by plateau uplift in southern Asia and the American west, Atmospheres, 94, 18409–18427, doi:10.1029/JD094iD15p18409, 1989.

Rühlemann, C., Müller, P. J., and Schneider, R. R.: Organic carbon and carbonate as paleoproductivity proxies: Examples from high and low productivity areas of the tropical Atlantic. In: Fischer, G. and Wefer, G. (Eds), Use of proxies in paleoceanography: Examples from the South Atlantic. Springer, Berlin, Heidelberg, 315–344, 1999.

Sarkar, S. and Gupta, A. K.: Deep-sea paleoceanography of Maldives Islands (ODP Hole 716A), equatorial Indian Ocean during MIS 12-6, Journal of Bioscience, 34, 749–764, doi:10.1007/s12038-009-0066-7, 2009.

Sarkar, S. and Gupta, A. K.: Late Quaternary productivity changes in the equatorial Indian Ocean (ODP Hole 716A), Palaeogeography, Palaeoclimatology, Palaeoecology, 397, 7–19, doi:10.1016/j.palaeo.2013.12.002, 2014.

Sasamal, S. K.: Island wake circulation off Maldives during boreal winter, as visualised with MODIS derived chlorophyll-a data and other satellite measurements, International Journal of Remote Sensing, 28, 891–903, doi:10.1080/01431160600858459, 2007.

Schlager, W., Reijmer, J. J. G., and Droxler, A.: Highstand Shedding of Carbonate Platforms, Journal of Sedimentary Research, 64B, 270–281, 1994.

Schmiedl, G., Mackensen, A., and Müller, P. J.: Recent benthic foraminifera from the eastern South Atlantic Ocean: Dependence on food supply and water masses, Marine Micropaleontology, 32, 249–287, doi:10.1016/S0377-8398(97)00023-6, 1997.

Schmiedl, G. and Leuschner, D. C.: Oxygenation changes in the deep western Arabian Sea during the last 190,000 years: productivity versus deep-water circulation, Paleoceanography, 20, PA2008, 1–14, doi:10.1029/2004PA001044, 2005.

Schmiedl, G. and Mackensen, A.: Multispecies stable isotopes of benthic foraminifers reveal past changes of organic matter decomposition and deepwater oxygenation in the Arabian Sea, Paleoceanography, 21, PA4213, 1–14, doi:10.1029/2006PA001284, 2006.

Schoepfer, S. D., Shen, J., Wei, H., Tyson, R. V., Ingall, E., and Algeo, T. J.: Total organic carbon, organic phosphorus, and biogenic barium fluxes as proxies for paleomarine productivity, Earth-Science Reviews, 149, 23–52, doi:10.1016/j.earscirev.2014.08.017, 2015.

Schott, F. A. and McCreary Jr., J. P.: The monsoon circulation of the Indian Ocean, Progress in Oceanography, 51, 1–123, doi:10.1016/S0079-6611(01)00083-0, 2001.

Schulz, H., von Rad, U., and Erlenkeuser, H.: Correlation between Arabian Sea and Greenland climate oscillation of the past 110,000 years, Nature, 393, 54–57, doi:10.1038/31750, 1998.

Singh, A. D., Jung, S. J. A., Darling, K., Ganeshram, R., Ivanochko, T., and Kroon, D.: Productivity collapses in the Arabian Sea during glacial cold phases, Paleoceanography, 26, PA3210, 1–10, doi:10.1029/2009PA001923, 2011.

Sirocko, F. and Lange, H.: Clay-mineral accumulation rates in the Arabian Sea during the late Quaternary, Marine Geology, 97, 105–119, doi:10.1016/0025-3227(91)90021-U, 1991.

Smith, A. J. and Gallagher, S. J.: The Recent foraminifera and facies of the Bass Canyon: a temperate submarine canyon in Gippsland, Australia, Journal of Micropalaeontology, 22, 63–83, doi:10.1144/jm.22.1.63, 2003.

Southon, J., Kashgarian, M., Fontugne, M., Metivier, B., and Yim, W. W.-S.: Marine Reservoir Corrections for the Indian Ocean and Southeast Asia, Radiocarbon, 44, 167–180, doi:10.1017/S0033822200064778, 2002.

Stramma, L., Johnson, G. C., Sprintall, J., and Mohrholz, V.: Expanding oxygen-minimum zones in the tropical oceans, Science, 320, 655–658, doi:10.1126/science.1153847, 2008.

Stuiver, M. and Reimer, P. J.: Extended ^{14}C data base and revised CALIB 3.0 ^{14}C age calibration program, Radiocarbon, 35, 215–230, 1993.

Sun, X., Corliss, B. H., Brown, C. W., and Showers, W. J.: The effect of primary productivity and seasonality on the distribution of deep-sea benthic foraminifera in the North Atlantic, Deep-Sea Research I, 53, 28–47, doi:10.1016/j.dsr.2005.07.003, 2006.

Thiede, J., Nees, S., Altenbach, A., Andresen, N., Findlay, C., Hill, P., Howard, W., Jellinek, T., Jurkschat, T., Laurent, E., van der Lingen, G., Müller, A., Neil, H., Probert, I., Rehder, W., Reijmer, J., Rendle, R., Roth, S., Rueggeberg, A., Runze, O., Schulz, H., Schumann, M., Sturm, A., Swanson, K., and Willamowski, C.: FS Sonne Fahrtbericht SO136, Cruise Report SO136, TASQWA: Quaternary variability of water masses in Southern Tasman sea and the southern ocean (SW pacific sector), Wellington-Hobart, October 16-November 12, GEOMAR Report 89, 1–106, GEOMAR, Kiel, 1999.

Weiss, R. F., Broecker, W. S., Craig, H., and Spencer, D.: GEOSECS Indian Ocean Expedition: Hydrographic Data 1977–1978, 5, U.S. Government Printing Office, Washington, D.C, 1–62, 1983.

Wiggert, J. D., Murtugudde, R. G., and Christian, J. R.: Annual ecosystem variability in the tropical Indian Ocean: Results of a coupled bio-physical ocean general circulation model, Deep Sea Research Part II, Topical Studies in Oceanography, 53, 644–676, doi:10.1016/j.dsr2.2006.01.027, 2006.

Wyrtki, K.: Physical oceanography of the Indian Ocean. In: Zeitzschel, B. and Gerlach, S. A. (Eds.), The biology of the Indian Ocean, Springer-Verlag, Berlin, Heidelberg, 18–36, 1973.

You, Y.: Intermediate water circulation and ventilation of the Indian Ocean derived from water-mass contributions, Journal of Marine Research, 56, 1029–1067, 1998.

Zhang, X., Arimoto, R., An, Z., Chen, T., Zhang, G., Zhu, G., and Wang, X.: Atmospheric trace elements over source regions for Chinese dust: concentrations, sources and atmospheric depositions on the Loess Plateau, Atmospheric Environment, 27A, 2051–2067, doi:10.1016/0960-1686(93)90277-6, 1993.

Zhang, X. Y., Lu, H. Y., Arimoto, R., and Gong, S. L.: Atmospheric dust loadings and their relationship to rapid oscillations of the Asian winter monsoon climate: two 250-ka loess records, Earth and Planetary Science Letters, 202, 637–643, doi:10.1016/S0012-821X(02)00797-5, 2002.

Ziegler, M., Jilbert, T., de Lange, G., Lourens, L. J., and Reichart, G.-J.: Bromine counts from XRF scanning as an estimate of the marine organic carbon content of sediment cores, Geochemistry, Geophysics, Geosystems, 9, 1–6, doi:10.1029/2007GC001932, 2008.

Ziegler, M., Lourens, L. J., Tuenter, E., and Reichart, G.-J.: Anomalously high Arabian Sea productivity conditions during MIS 13, Climate of the Past Discussions, 5, 1989–2018, 2009.

Ziegler, M., Lourens, L. J., Tuenter, E., and Reichart, G.-J.: High Arabian Sea productivity conditions during MIS 13 – odd monsoon event or intensified overturning circulation at the end of the Mid-Pleistocene transition?, Climate of the past, 6, 63–76, 2010.

Table Captions

Table 1: Accelerator Mass Spectrometry (AMS) radiocarbon dating results based on mixed surface-dwelling planktonic foraminifera (*Gr* = *Globigerinoides ruber*, white; *Gs* = *Globigerinoides sacculifer*) from 35 cm, 80 cm and 140 cm sediment depth of core SO236-052-4. Conventional radiocarbon ages were calibrated using the radiocarbon calibration program CALIB (version 7.0.4; Stuiver and Reimer, 1993) and the calibration curve Marine13 (Reimer et al., 2013).

No.	**Sample ID**	**Lab ID**	**Material**	**Core depth**	**^{12}C/ ^{13}C**	**^{14}C age**	**Calibrated age (ΔR 0)**		
							cal BP (2s ranges, 95.4 % probability)		
				[mbsf]	o/oo	ya BP	range [years]	rel. area u. distr.	median of prob. [ka]
1	SO236-052-035	Beta-418574	*Gr, Gs*	0.35	+1.4	7940 ±30	8330 - 8480	1.00	**8.4 ± 0.08**
2	SO236-052-080	Beta-418575	*Gr, Gs*	0.80	+1.6	12890 ±40	14310 - 15020	1.00	**14.7 ± 0.36**
3	SO236-052-140	Beta-418576	*Gr, Gs*	1.40	+1.8	23930 ±100	27480 - 27850	1.00	**27.7 ± 0.19**

Table 2: Species composition of benthic foraminiferal assemblages. Principal component number, dominant and important associated species with principal component scores (Q-mode) and explained variance in percent of total variance are given.

Q-mode Principal Components	Species	Scores	Explained variance [%]
PC1	***Neouvigerina proboscidea***	5.812	31.54
	Discorbinella araucana	3.948	
	Hyalinea inflata	2.562	
	Cymbaloporetta squammosa	1.913	
	Bulimina marginata	1.729	
	Rosalina vilardeboana	1.595	
PC2	***Cibicides mabahethi***	7.466	30.54
	Discorbinella bertheloti	1.756	
	Siphogenerina columellaris	1.622	
	Gyroidina umbonata	1.589	
	Reophax sp.	1.387	
	Hyalinea inflata	1.214	
	Discorbinella araucana	1.109	
PC3	***Neouvigerina proboscidea***	4.608	27.06
	Hoeglundina elegans	3.952	
	Discorbinella bertheloti	3.004	
	Cibicidoides subhaidingeri	2.311	
	Discorbis sp.	2.161	
	Spiroplectinella sagittula s.l.	1,808	
	Cibicides mabahethi	1,084	

Figure Captions

Figure 1: Location maps of the Maldives archipelago in the Indian Ocean (a, b) and the setting of the study area (c) (modified after Betzler et al., 2013a), showing the location of sediment core M74/4-1143 in the Kardiva Channel and core SO236-052-4 in the central part of the Inner Sea (red circles).

Figure 2: Full resolution stable oxygen isotope records of the planktonic foraminifer *G. ruber* (a) and age-depth plots for the sediment cores SO236-052-4 (light blue) and M74/4-1143 (grey). Orange triangles indicate radiocarbon dates and circles indicate age control points derived from correlation with the LR04 benthic isotope stack of Lisiecki and Raymo (2005). Sedimentation rates are derived from linear interpolation between age data. MIS denotes the Marine stable oxygen isotope stages.

Figure 3: a-b) Stable oxygen and carbon isotope records of planktonic and benthic foraminifera of sediment core SO236-052-4. Displayed are the planktonic species *G. ruber* (light blue), the epibenthic species *C. mabahethi* (dark blue) and the deep infaunal species *G. affinis* s.l. (red). Also shown are the full-resolution data of the $\Delta\delta^{13}C_{Gr\text{-}Cm}$ and $\Delta\delta^{13}C_{Cm\text{-}Ga}$ signals (c), as a result of the difference between the $\Delta\delta^{13}C$ values of *G. ruber* and *C. mabahethi*, as well as *C. mabahethi* and *G. affinis* s.l. MIS denotes the Marine stable oxygen isotope stages.

Figure 4: Records and normalized Blackman-Tukey power spectra of a, b) the oxygen reconstructions of core SO236-052-4 (blue) and GeoB3004 (purple), c, d) productivity proxies TOC (green) and Br XRF counts (pink), and e, f) dust proxies Ti/Al (light blue) and Fe/Al (dark blue), in comparison to the Δ-insolation at 30° N (black dashed line). Grey bars indicate the 23 ka period of the Δ-insolation and its band width. Oxygen and TOC records represent five-point running averages, Br XRF counts, Ti/Al and Fe/Al records represent fifteen-point running averages.

Figure 5: Sedimentological and geochemical records of sediment core SO236-052-4 from the central part of the Maldives Inner Sea. a) Sortable silt (black) in comparison with the data of core M74/4-1143 (brown) and bulk sediment (grey) MEAN values, b) total organic carbon (TOC) (dark green) and calcium carbonate (light green) content of the sediment, c) iron (dark blue) and titanium (light blue) in relation to the aluminium XRF counts, and d) bromine XRF counts (pink), and silicon (dark purple) and strontium (light purple) in relation to the calcium XRF counts. Thin lines represent full-resolution data, bold lines in a) and b) indicate five-point running averages, whereas all XRF counts in c) and d) are displayed as a fifteen-point running average (bold lines). MIS denotes the Marine stable oxygen isotope stages.

Figure 6: a) Epibenthic stable oxygen isotope record of core SO236-052-4 (dark blue) in comparison with the LR04 benthic stable isotope stack (orange; Lisiecki and Raymo, 2005). b-c) Comparison of the sortable silt records of sediment cores M74/4-1143 and SO236-052-4, and d) relative abundance of meroplanktonic benthic foraminifera (BF; including the genera *Cymbaloporetta* and *Tretomphaloides*) in sediments of core SO236-052-4. Thin lines represent full-resolution data, bold lines indicate five-point running averages. MIS denotes the Marine stable oxygen isotope stages.

Figure 7: Comparison of benthic foraminiferal faunal records of core SO236-052-4 from the central part of the Maldives Inner Sea. a) Shannon-Wiener diversity index H(S), b-d) Q-mode benthic foraminiferal assemblages, including the *N. proboscidea-/D. araucana*-fauna (assemblage 1), the *C. mabahethi*-fauna (assemblage 2), and the *N. proboscidea-/H. elegans*-fauna (assemblage 3). Loadings ≥ 0.5 are defined as significant after Backhaus et al. (2008). e-g) Distribution of selected important and associated benthic foraminiferal taxa, given in percent. The meroplanktonic benthic foraminifera (BF) comprise the genera *Cymbaloporetta* and *Tretomphaloides*.

Figure 8: Variation of the insolation difference between the June and December solstice at 30° N (after Laskar, 2004; calculated with AnalySeries 2.0: Paillard et al. 1996) (a) in graphical correlation with geochemical and benthic foraminiferal productivity records of core SO236-052-4. b) Total organic carbon (TOC) content and c) Bromine as derived from XRF scanning count data as tracer for marine organic carbon (MOC), d) Fe/Al ratio and e) relative abundance of agglutinated benthic foraminifera as indicator for enhanced dust supply. f) Principal Components (PC) show the *C. mabahethi*-fauna (assemblage 2) and *N. proboscidea*-/*H. elegans*-fauna (assemblage 3). This comparison reveals coherent glacial-to-interglacial changes in all proxy records with elevated values during glacial stages MIS 6 and MIS 4-2 and during a weaker northern hemisphere solar radiation-amplitude (yellow bars). Thin lines represent full-resolution data, bold lines in b) and e) indicate five-point running averages, bold lines in c) and d) indicate a fifteen-point running average. MIS denotes the Marine stable oxygen isotope stages.

Figure 9: Water mass circulation changes obtained from stable δ^{13}C data of core SO236-052-4 (Indian Ocean) in comparison to ventilation changes in the Arabian Sea. a) δ^{13}C records of the planktonic *G. ruber* (light blue) and the epibenthic *C. mabahethi* (dark blue), b) difference between the planktonic and epibenthic stabile carbon records ($\Delta\delta^{13}C_{Gr-Cm}$), c) differences between epibenthic and deep endobenthic δ^{13}C records of SO236-052-4 (dark blue) from the intermediate Maldives Inner Sea in comparison to that of GeoB3004 (purple) from the deep Arabian Sea (Schmiedl and Mackensen, 2006). Changes in intermediate- and deep-water oxygen concentrations are calculated by the linear regression between the $\Delta\delta^{13}$C and $[O_2] < 235$ µmol kg^{-1} after Hoogakker et al. (2015). Minimum significance level of $[O_2] = 55$ µmol kg^{-1} is shown as dashed line (Hoogakker et al., 2015). Variation of the insolation difference between the June and December solstice at 30° N (yellow) were estimated after Laskar (2004) with AnalySeries 2.0 (Paillard et al., 1996). All lines indicate five-point running averages. MIS denotes the Marine stable oxygen isotope stages. *Cib.* = *Cibicides*, *Cm* = *Cibicides mabahethi*, *Cw* = *Cibicides wuellerstorfi*, *Ga* = *Globobulimina affinis*, *Gr* = *Globigerinoides ruber*.

Figure 10: Comparison of epibenthic δ^{13}C records from intermediate water depth of the equatorial Indian and temperate southwestern Pacific Ocean. a) δ^{13}C record of *C. mabahethi* (blue) from the Maldives Inner Sea (SO236-052) in comparison to δ^{13}C records from the southwestern Pacific Ocean, which were mainly generated from *Cibicidoides wuellerstorfi*, *C. cicatricosa* and *C. kullenbergi* and represent different water depths (Thiede et al., 1999; Pahnke and Zahn, 2005; Elmore et al., 2015; Ronge et al., 2015). Data of MD97-2120 were traced after Pahnke and Zahn (2005). All lines represent five-point running averages. b) Simplified map of the Indian Ocean and the southwestern Pacific Ocean with location of the study sites.

Figure 1

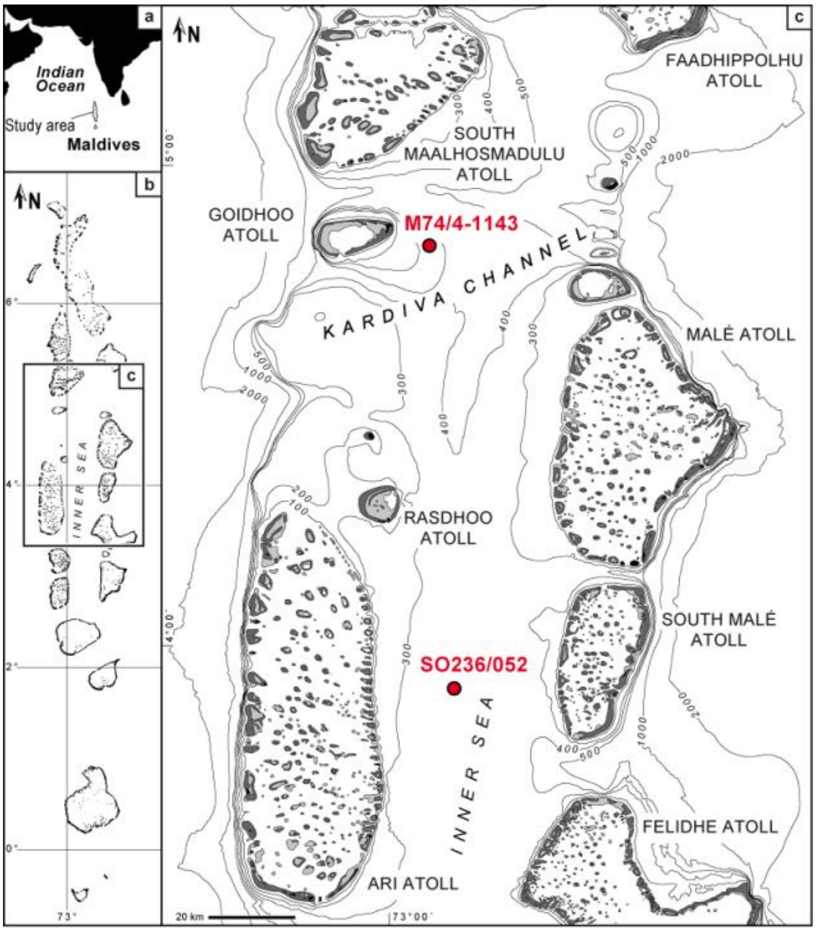
a
Indian Ocean
Study area
Maldives
b
N
6°
4°
2°
0°
73°
c
INNER SEA
N
FAADHIPPOLHU ATOLL
SOUTH MAALHOSMADULU ATOLL
GOIDHOO ATOLL
M74/4-1143
KARDIVA CHANNEL
MALÉ ATOLL
RASDHOO ATOLL
SOUTH MALÉ ATOLL
SO236/052
INNER SEA
FELIDHE ATOLL
ARI ATOLL
5°00'
4°00'
73°00'
20 km
100
200
300
400
500
1000
2000

Figure 2

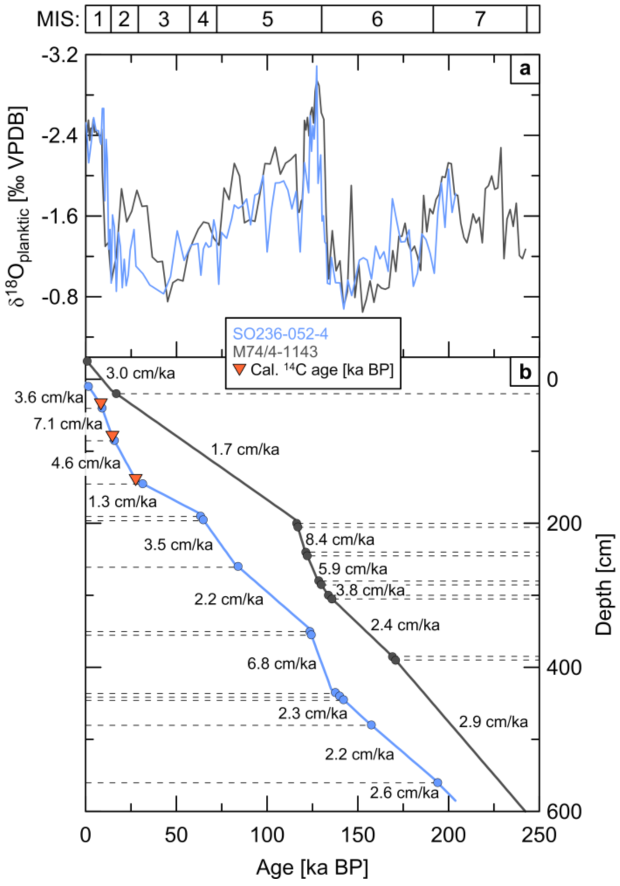

MIS:
1
2
3
4
5
6
7
a
-3.2
-2.4
-1.6
-0.8
$\delta^{18}O_{planktic}$ [‰ VPDB]
SO236-052-4
M74/4-1143
▼ Cal. ^{14}C age [ka BP]
b
3.0 cm/ka
3.6 cm/ka
7.1 cm/ka
4.6 cm/ka
1.3 cm/ka
1.7 cm/ka
3.5 cm/ka
8.4 cm/ka
5.9 cm/ka
3.8 cm/ka
2.2 cm/ka
2.4 cm/ka
6.8 cm/ka
2.3 cm/ka
2.9 cm/ka
2.2 cm/ka
2.6 cm/ka
0
200
400
600
Depth [cm]
0
50
100
150
200
250
Age [ka BP]

Figure 3

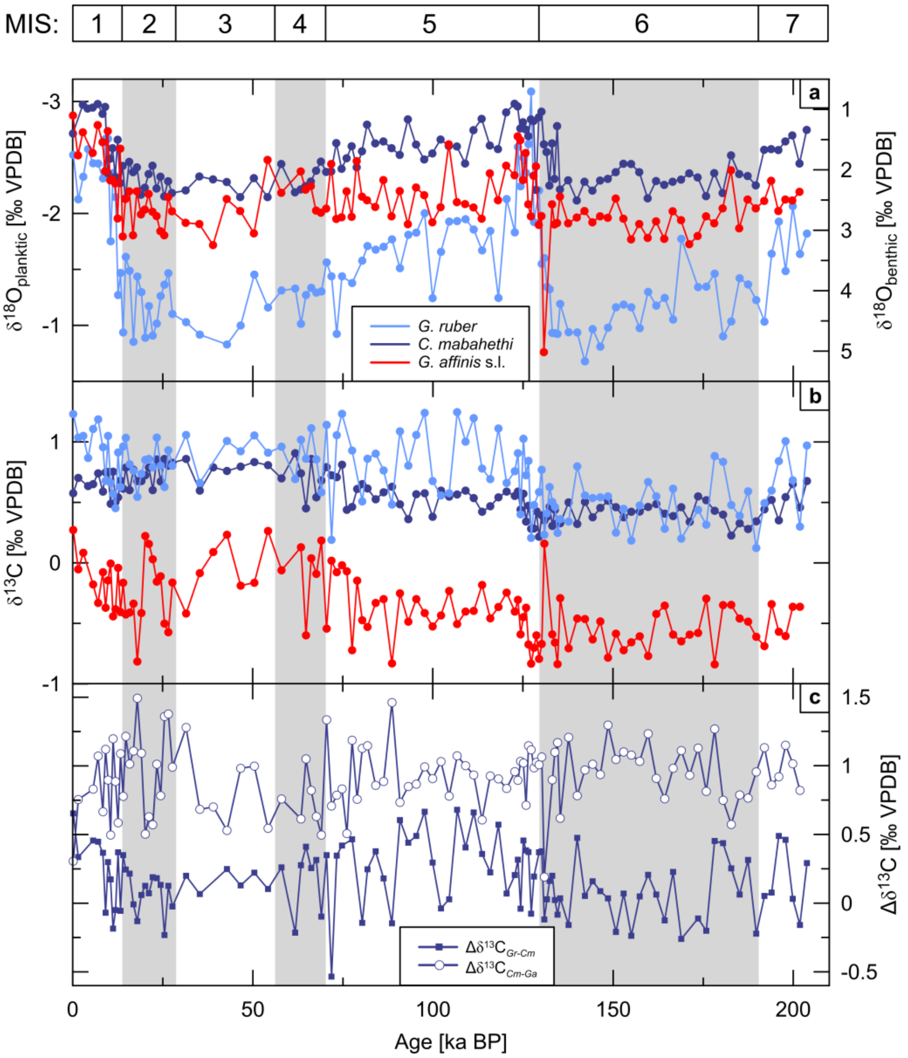
MIS:
1
2
3
4
5
6
7
a
b
c
$\delta^{18}O_{planktic}$ [‰ VPDB]
-3
-2
-1
$\delta^{18}O_{benthic}$ [‰ VPDB]
1
2
3
4
5
G. ruber
C. mabahethi
G. affinis s.l.
$\delta^{13}C$ [‰ VPDB]
1
0
-1
$\Delta\delta^{13}C$ [‰ VPDB]
1.5
1
0.5
0
-0.5
$\Delta\delta^{13}C_{Gr-Cm}$
$\Delta\delta^{13}C_{Cm-Ga}$
0
50
100
150
200
Age [ka BP]

Figure 4

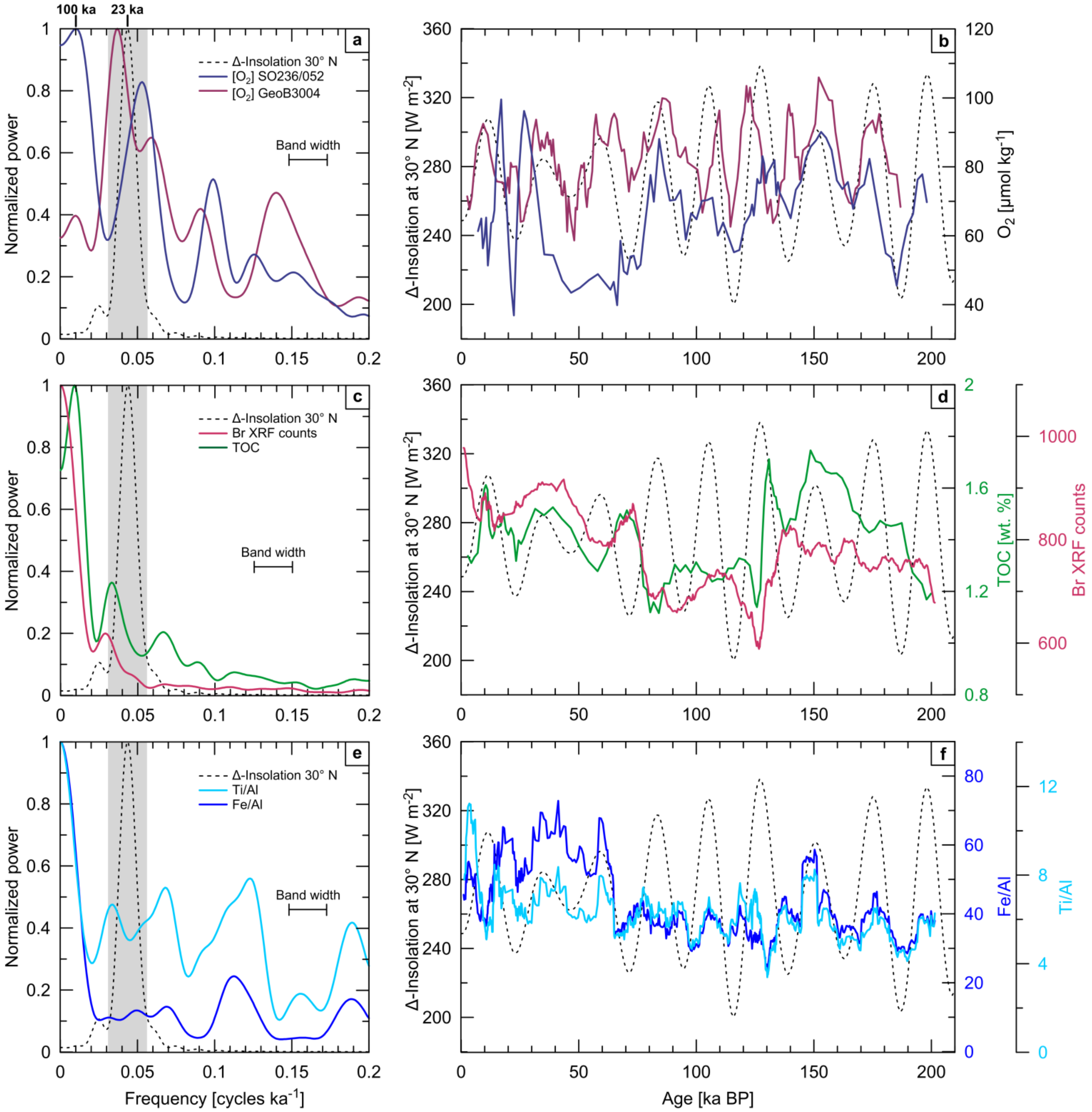

100 ka
23 ka
a
Δ-Insolation 30° N
[O$_2$] SO236/052
[O$_2$] GeoB3004
Band width
Normalized power
b
Δ-Insolation at 30° N [W m^{-2}]
O$_2$ [µmol kg^{-1}]
c
Δ-Insolation 30° N
Br XRF counts
TOC
Band width
Normalized power
d
Δ-Insolation at 30° N [W m^{-2}]
TOC [wt. %]
Br XRF counts
e
Δ-Insolation 30° N
Ti/Al
Fe/Al
Band width
Normalized power
Frequency [cycles ka^{-1}]
f
Δ-Insolation at 30° N [W m^{-2}]
Fe/Al
Ti/Al
Age [ka BP]
0
0.05
0.1
0.15
0.2
0
0.2
0.4
0.6
0.8
1
0
50
100
150
200
200
240
280
320
360
40
60
80
100
120
0.8
1.2
1.6
2
600
800
1000
0
20
40
60
80
0
4
8
12

Figure 5

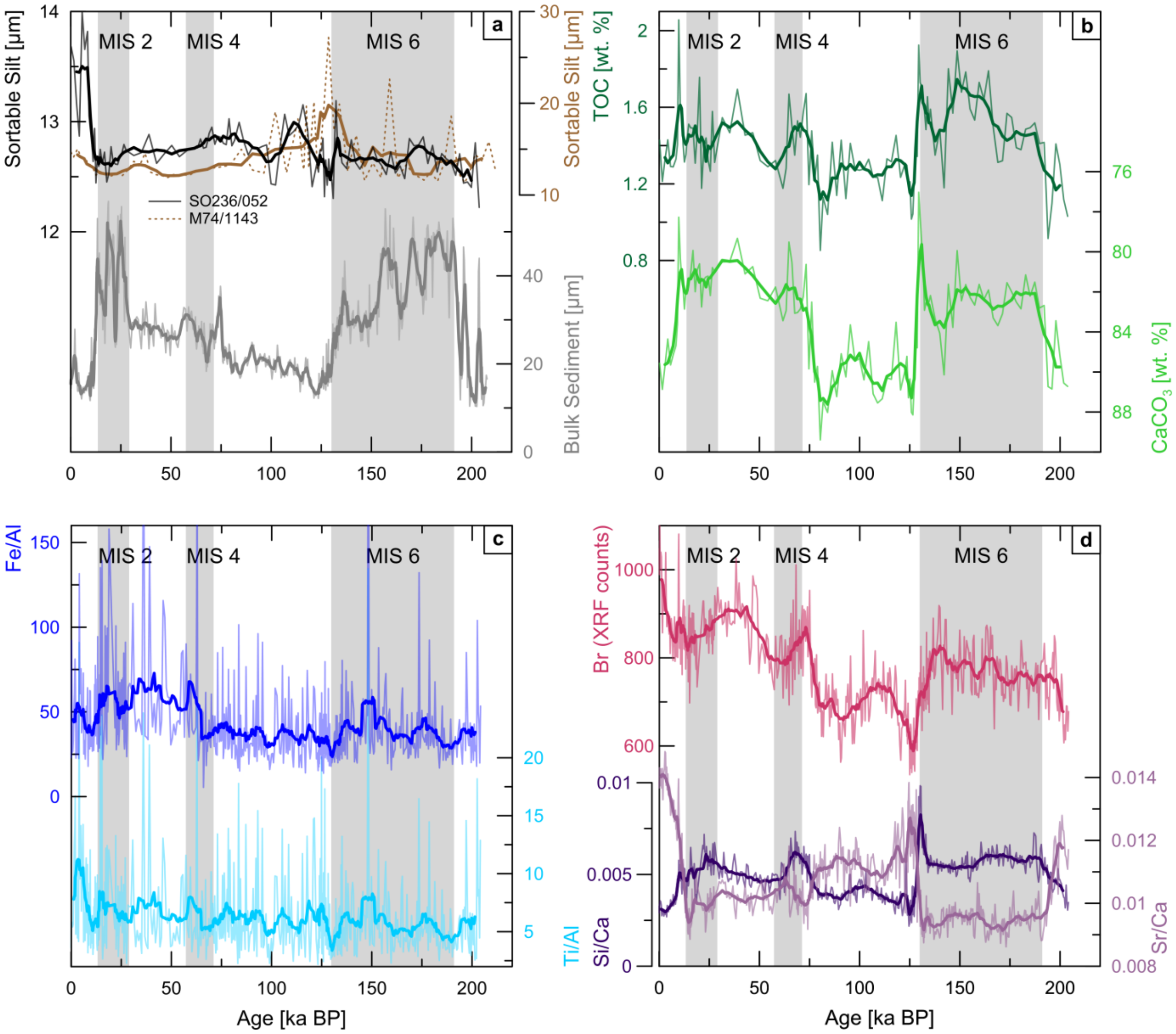
a
b
c
d
MIS 2
MIS 4
MIS 6
Sortable Silt [µm]
14
13
12
Sortable Silt [µm]
30
20
10
SO236/052
M74/1143
Bulk Sediment [µm]
40
20
0
TOC [wt. %]
2
1.6
1.2
0.8
CaCO$_3$ [wt. %]
76
80
84
88
Fe/Al
150
100
50
0
Ti/Al
20
15
10
5
Br (XRF counts)
1000
800
600
Si/Ca
0.01
0.005
0
Sr/Ca
0.014
0.012
0.01
0.008
0
50
100
150
200
Age [ka BP]

Figure 6

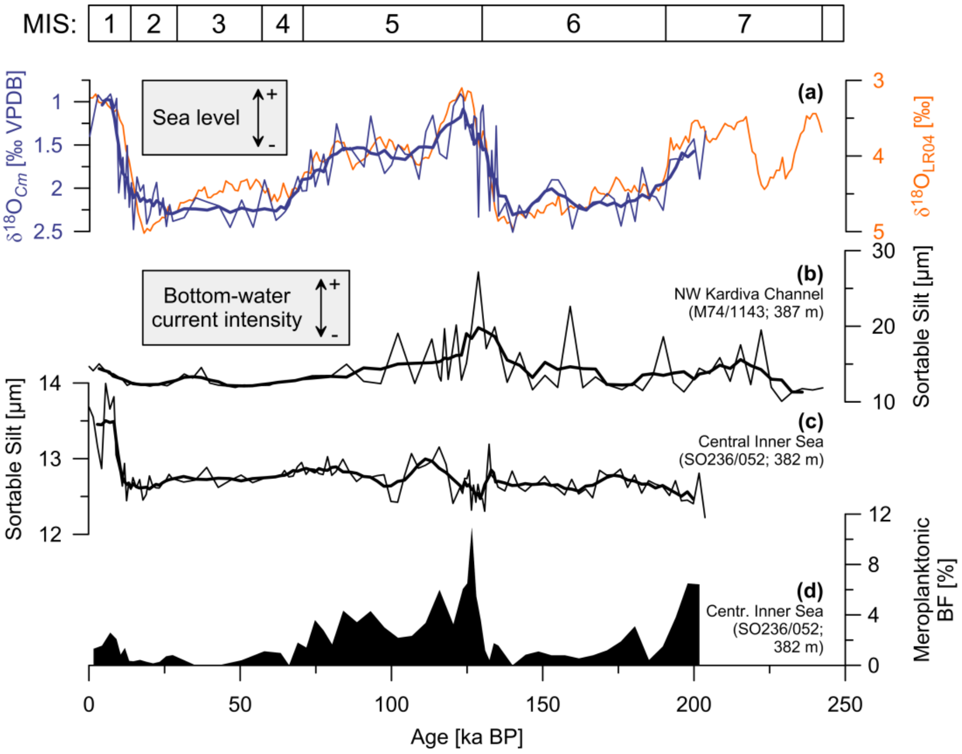
MIS:
1
2
3
4
5
6
7
Sea level
+
-
(a)
$\delta^{18}O_{Cm}$ [‰ VPDB]
1
1.5
2
2.5
3
4
5
$\delta^{18}O_{LR04}$ [‰]
Bottom-water current intensity
+
-
(b)
NW Kardiva Channel
(M74/1143; 387 m)
30
20
10
Sortable Silt [µm]
14
13
12
Sortable Silt [µm]
(c)
Central Inner Sea
(SO236/052; 382 m)
(d)
Centr. Inner Sea
(SO236/052;
382 m)
12
8
4
0
Meroplanktonic BF [%]
0
50
100
150
200
250
Age [ka BP]

Figure 7

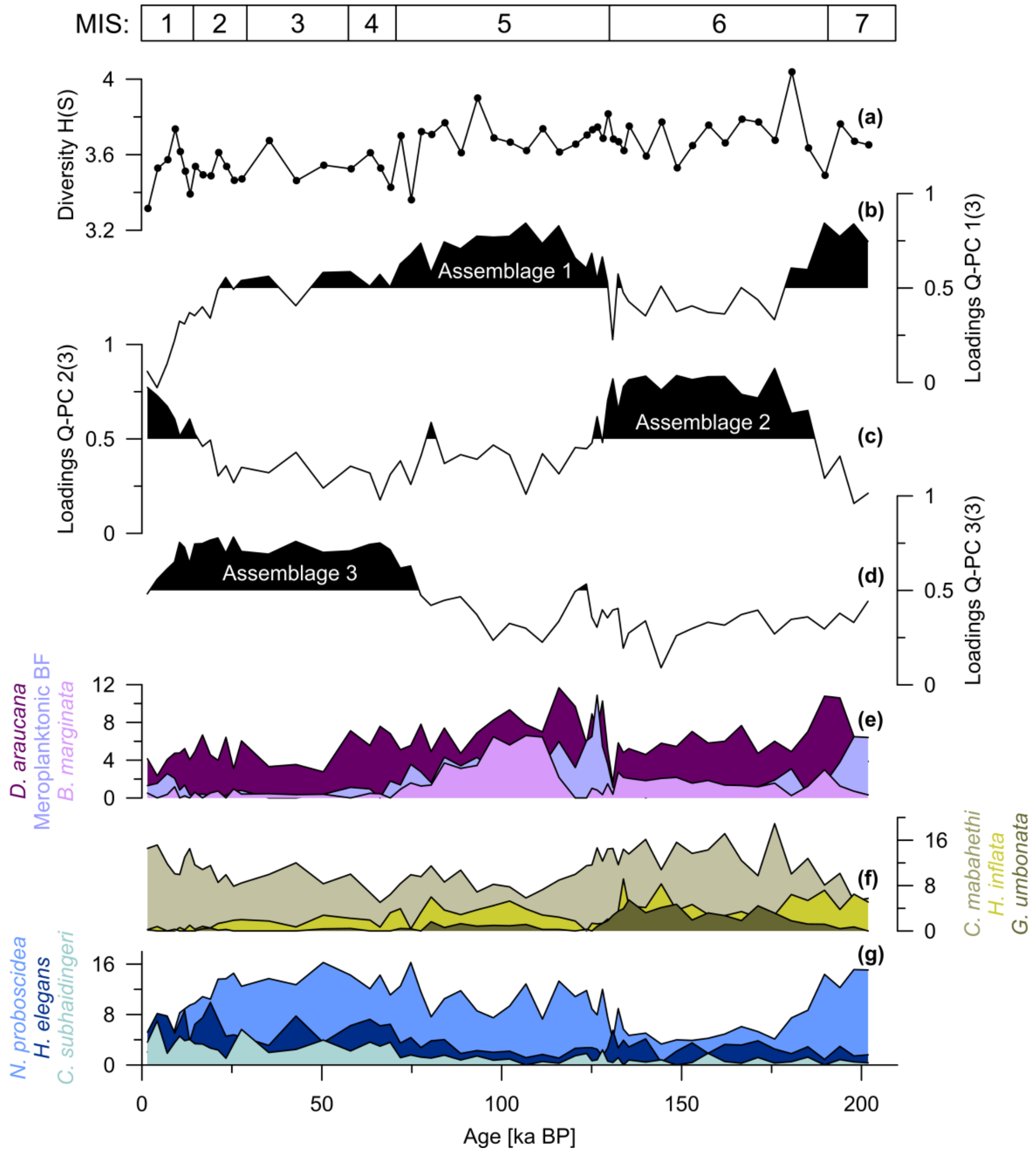
MIS:
1
2
3
4
5
6
7
Diversity H(S)
4
3.6
3.2
(a)
(b)
1
0.5
0
Loadings Q-PC 1(3)
Assemblage 1
Loadings Q-PC 2(3)
1
0.5
0
Assemblage 2
(c)
Assemblage 3
(d)
Loadings Q-PC 3(3)
1
0.5
0
D. araucana
Meroplanktonic BF
B. marginata
12
8
4
0
(e)
(f)
16
8
0
C. mabahethi
H. inflata
G. umbonata
N. proboscidea
H. elegans
C. subhaidingeri
(g)
16
8
0
0
50
100
150
200
Age [ka BP]

Figure 8

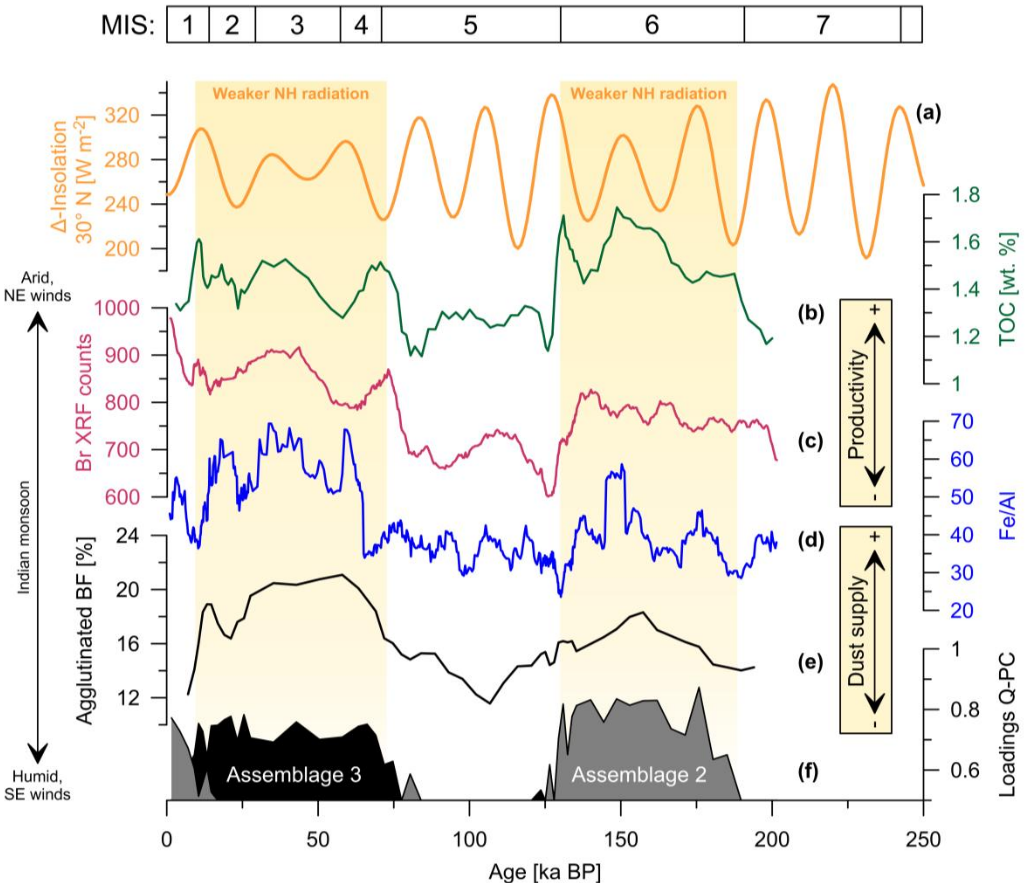
MIS:
1
2
3
4
5
6
7
Weaker NH radiation
Weaker NH radiation
Δ-Insolation 30° N [W m⁻²]
320
280
240
200
(a)
1.8
1.6
1.4
1.2
1
TOC [wt. %]
Arid, NE winds
Humid, SE winds
Indian monsoon
Br XRF counts
1000
900
800
700
600
(b)
(c)
Productivity
+
-
70
60
50
40
30
20
Fe/Al
(d)
Dust supply
+
-
Agglutinated BF [%]
24
20
16
12
(e)
1
0.8
0.6
Loadings Q-PC
Assemblage 3
Assemblage 2
(f)
0
50
100
150
200
250
Age [ka BP]

Figure 9

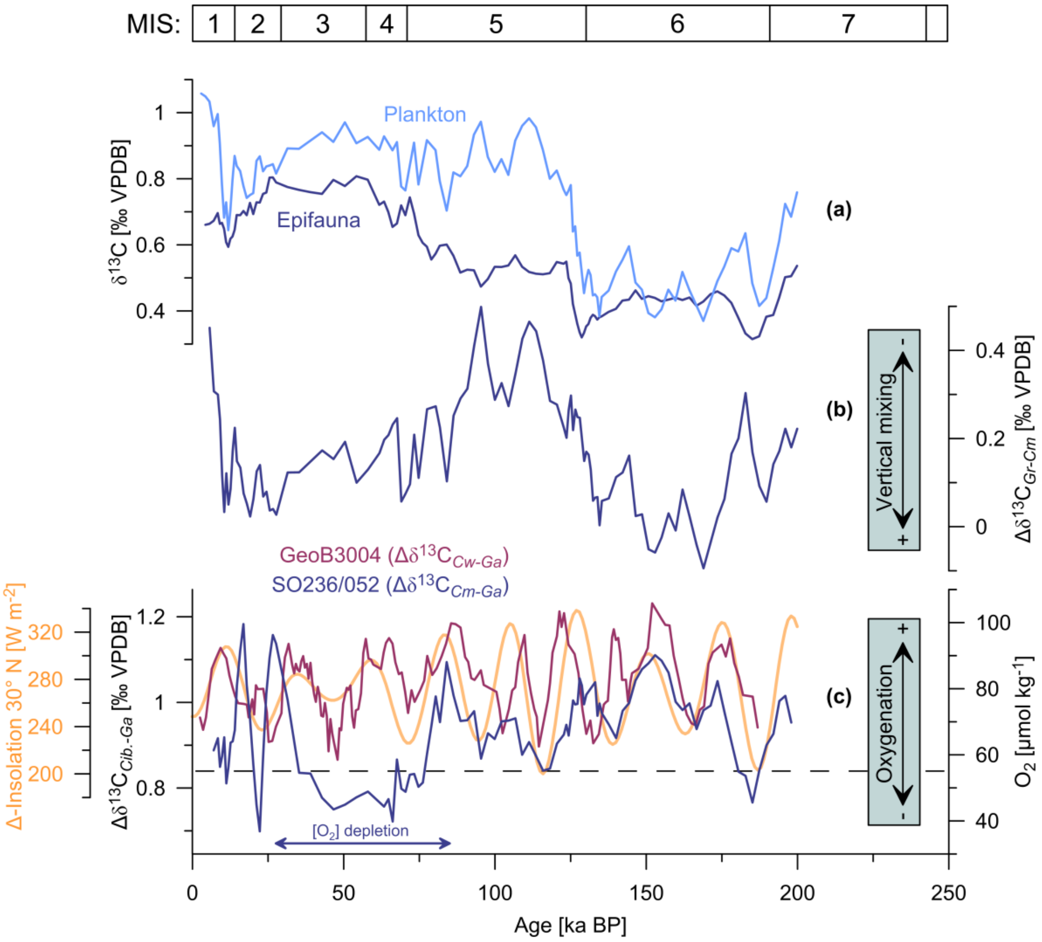
MIS:
1
2
3
4
5
6
7
Plankton
Epifauna
$\delta^{13}C$ [‰ VPDB]
1
0.8
0.6
0.4
(a)
(b)
Vertical mixing
-
+
0.4
0.2
0
$\Delta\delta^{13}C_{Gr-Cm}$ [‰ VPDB]
GeoB3004 ($\Delta\delta^{13}C_{Cw-Ga}$)
SO236/052 ($\Delta\delta^{13}C_{Cm-Ga}$)
Δ-Insolation 30° N [W m^{-2}]
320
280
240
200
$\Delta\delta^{13}C_{Cib.-Ga}$ [‰ VPDB]
1.2
1
0.8
(c)
Oxygenation
+
-
100
80
60
40
O_2 [µmol kg^{-1}]
[O_2] depletion
0
50
100
150
200
250
Age [ka BP]

Figure 10

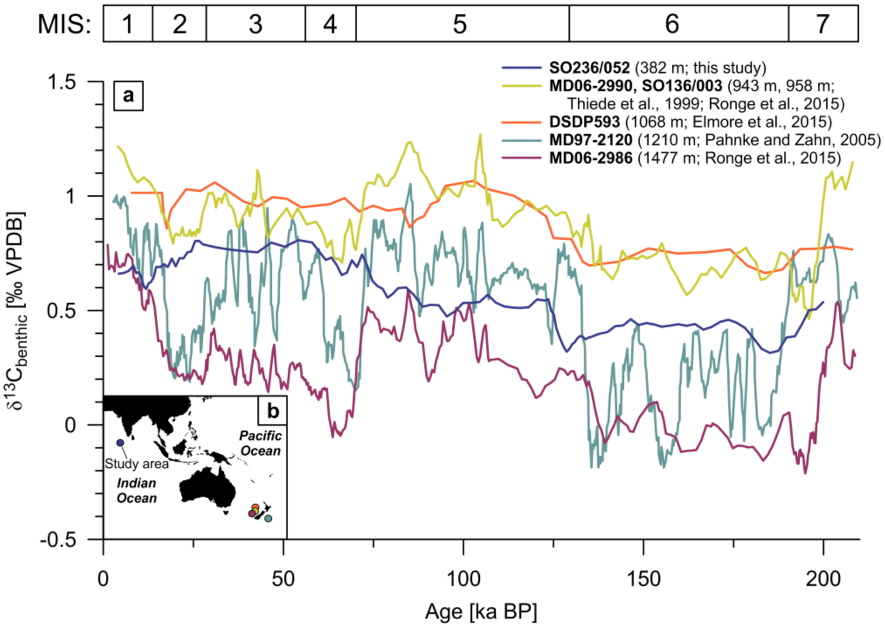
MIS:
1
2
3
4
5
6
7
a
SO236/052 (382 m; this study)
MD06-2990, SO136/003 (943 m, 958 m; Thiede et al., 1999; Ronge et al., 2015)
DSDP593 (1068 m; Elmore et al., 2015)
MD97-2120 (1210 m; Pahnke and Zahn, 2005)
MD06-2986 (1477 m; Ronge et al., 2015)
1.5
1
0.5
0
-0.5
$\delta^{13}C_{benthic}$ [‰ VPDB]
b
Study area
Indian Ocean
Pacific Ocean
0
50
100
150
200
Age [ka BP]